5-2012

# Role of TRP Channels in Mediating the Calcium Signaling Response of Brain Endothelial Cells to Mechanical Stretch

Jonathan Berrout

# Role of TRP Channels in Mediating the Calcium Signaling Response of Brain Endothelial Cells to Mechanical Stretch

A

DISSERTATION

Presented to the Faculty of

The University of Texas Health Science Center at Houston

and

The University of Texas M. D. Anderson Cancer Center

Graduate School of Biomedical Sciences

In Partial Fulfillment the Requirements for

The Degree of

**DOCTOR OF PHILOSOPHY**

**by**

**Jonathan Berrout, B.S.**

Houston, Texas

May 2012

**Role of TRP Channels in Mediating the Calcium Signaling Response of Brain Endothelial Cells to Mechanical Stretch**

By

**Jonathan Berrout, B.S.**

APPROVED:

_____ Chair
[Roger G. O'Neil, PhD, Advisor]

_____
[Edgar T. Walters, PhD]

_____
[Pramod Dash, PhD]

_____
[Raymond Grill, PhD]

_____
[Hongzhen Hu, PhD]

APPOVED:

_____
Dean, The University of Texas
Health Science Center at Houston
Graduate School of Biomedical Sciences

## Dedication

This work is dedicated to my parents, Juan and Francis Berrout.

## Acknowledgments

I want to express my gratitude to Dr. Roger G. O'Neil for offering me the great opportunity to do my dissertation research in his laboratory. Dr. O'Neil has been a great mentor providing guidance and support to further my scientific and professional development. I'm grateful for the chance I received to learn new techniques and to attend many scientific conferences. I would also like to thank the members of my advisory and supervisory committees for their help in providing structure to my project. Finally, I would like to extend my thanks to all previous members of the lab: Rachel, Jose, Kali, Ling, and Min for all their help and friendship.

Role of TRP Channels in Mediating the Calcium Signaling Response of Brain Endothelial Cells to Mechanical Stretch

Publication No. _____

Jonathan Berrout, Ph.D.

Supervisory Professor: Roger G. O'Neil, Ph.D.

Traumatic brain injury (TBI) often results in disruption of the blood brain barrier (BBB), which is an integral component to maintaining the central nervous system homeostasis. Recently cytosolic calcium levels ($[Ca^{2+}]i$), observed to elevate following TBI, have been shown to influence endothelial barrier integrity. However, the mechanism by which TBI-induced calcium signaling alters the endothelial barrier remains unknown. In the present study, an *in vitro* BBB model was utilized to address this issue. Exposure of cells to biaxial mechanical stretch, in the range expected for TBI, resulted in a rapid cytosolic calcium increase. Modulation of intracellular and extracellular $Ca^{2+}$ reservoirs indicated that $Ca^{2+}$ influx is the major contributor for the $[Ca^{2+}]i$ elevation. Application of

pharmacological inhibitors was used to identify the calcium-permeable channels involved in the stretch-induced $Ca^{2+}$ influx. Antagonist of transient receptor potential (TRP) channel subfamilies, TRPC and TRPP, demonstrated a reduction of the stretch-induced $Ca^{2+}$ influx. RNA silencing directed at individual TRP channel subtypes revealed that TRPC1 and TRPP2 largely mediate the stretch-induced $Ca^{2+}$ response. In addition, we found that nitric oxide (NO) levels increased as a result of mechanical stretch, and that inhibition of TRPC1 and TRPP2 abolished the elevated NO synthesis. Further, as myosin light chain (MLC) phosphorylation and actin cytoskeleton rearrangement are correlated with endothelial barrier disruption, we investigated the effect mechanical stretch had on the myosin-actin cytoskeleton. We found that phosphorylated MLC was increased significantly by 10 minutes post-stretch, and that inhibition of TRP channel activity or NO synthesis both abolished this effect. In addition, actin stress fibers formation significantly increased 2 minutes post-stretch, and was abolished by treatment with TRP channel inhibitors. These results suggest that, in brain endothelial cells, TRPC1 and TRPP2 are activated by TBI-mechanical stress and initiate actin-myosin contraction, which may lead to disruption of the BBB.

## Table of Contents

## List of Tables

**List of Figures**

# Chapter 1: Introduction

## Blood Brain Barrier

At the level of the cerebral capillaries, the blood brain barrier (BBB) helps to maintain the homeostasis of the central nervous system through regulation of microvascular permeability. The barrier is composed of a monolayer of polarized endothelial cells which form the walls of cerebral capillaries (1-3). Surrounding the microvessel endothelial cells is a network of cells, together know as the neurovascular unit, that regulate the endothelial barrier and indirectly control microvascular permeability (Figure 1.1). The endothelial cells are exposed to two distinct environments; one being on the luminal surface exposed to blood and its constituents, while the other being on the abluminal surface exposed to the CNS interstitial fluid. On its abluminal surface, endothelial cells are ensheathed by the basal lamina, a matrix of extracellular proteins, composed primarily by laminin and collagen (5). Pericytes and astrocytic endfeet form close association with endothelial cells and regulate the barrier through the release of various cytokines and other signaling molecules (6-8). For instance, release of pro-angiogenic factor, vascular endothelial growth factor A, by astrocytes leads to loosening of the endothelial tight junctions and initiates remodeling of the microvascular tree. Further, cytokines interleukin-1, interleukin-6, and tumor necrosis factor alpha mediate a disruption of the endothelial barrier integrity and increase paracellular permeability; while release of angiopoietin 1 by pericytes mediates increased stability of the endothelial barrier (9-10). With no obvious interruptions along the

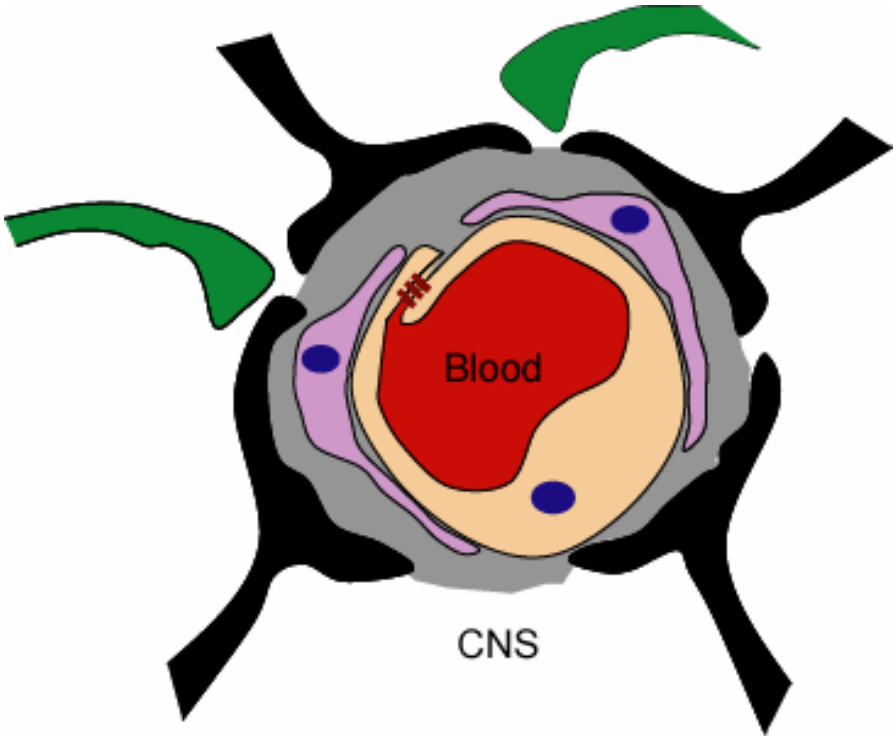


**Figure 1.1**. **Neurovascular Unit.**
Cross sectional representation of a cerebral capillary. In which, an endothelial cell (tan) forms the wall of the capillary and separates the blood from the CNS. In close proximity to the endothelial cell are pericytes (purple), astrocytic endfeet (black), and neuronal projections (green). The basal lamina is depicted in grey. Cell junctions expressed by the endothelial cell are shown as brown lines.

vessel wall, aside from the interendothelial cleft, brain capillaries resemble those found in heart, skeletal muscle and lung. However, despite similarities the permeability across brain capillaries is much more restrictive in comparison to other endothelia (11-13). Fittingly, the BBB was first identified by early studies describing that injection of dyes into the circulatory system failed to stain the brain and spinal cord while staining other organs; correspondingly dyes injected into the cerebral spinal fluid stained the brain but not other organs (11, 14). Although still not well understood, the need for a tight brain endothelial barrier may arise as a means to protect neurons (from toxins and molecules residing in the blood) and to strictly control neuronal activity (through fine control of ionic concentrations around synapses) (11, 15-16).

**Permeability across BBB**

Although initially considered to be a static barrier, today the BBB is regarded as a dynamic structure which continuously regulates microvascular permeability. This semi-permeable barrier allows the free passage of gases (O2 and CO2) and low molecular weight (<500) lipid-soluble substrates, while displaying low permeability to polar solutes (11, 13, 17). The primary properties contributing to the unique permeability of brain microvessel endothelial cells are its ability to act as a physical barrier by restricting paracellular permeability and its ability to act as a transport barrier by permitting the transcellular permeability only to select molecules (18-20). The transport barrier is made up by a network

of transporters and pumps which serve to move selected-molecules across the endothelium while extruding those molecules deemed undesirable. Some notable examples of transporters contributing to this aspect of barrier regulation are the P-glycoprotein (P-gp) and the organic anion transporting polypeptide 1A2 (OATP1A2) (21-23). The P-gp is an ATP-binding efflux transporter expressed on the luminal membrane of brain microvessel endothelial cells. It is well suited for mediating resistance to many chemotherapeutic drugs. OATP1A2 is a transporter also expressed on the luminal membrane of brain microvessel endothelial cells, and displays a broad substrate spectrum. The efficacy of the transport barrier to dictate molecular passage across the BBB is coupled to a "stinginess" of paracellular permeability, established by the physical barrier, obligating transcellular passage of molecules. The physical barrier is reliant on the expression and localization of specialized junctional complexes, tight junctions, which promote a tight relationship between endothelial membranes (Figure 1.2). Tight junction proteins occludin, claudin (1, 3, 5, and 12), and junctional adhesion molecule (JAM-A, B, and C) are found on brain microvessel endothelial cells (1, 24-25). Occludin is an integral membrane protein consistently detected along the margin of brain microvessel endothelial cells. It contains multiple phosphorylation sites believed to regulate its localization to the cell membrane and barrier permeability (26-29). Alteration of occludin expression is associated with BBB disruption under several disease states (30-32). Indeed, a decrease in occludin expression is reported to occur under hypoxia-induced

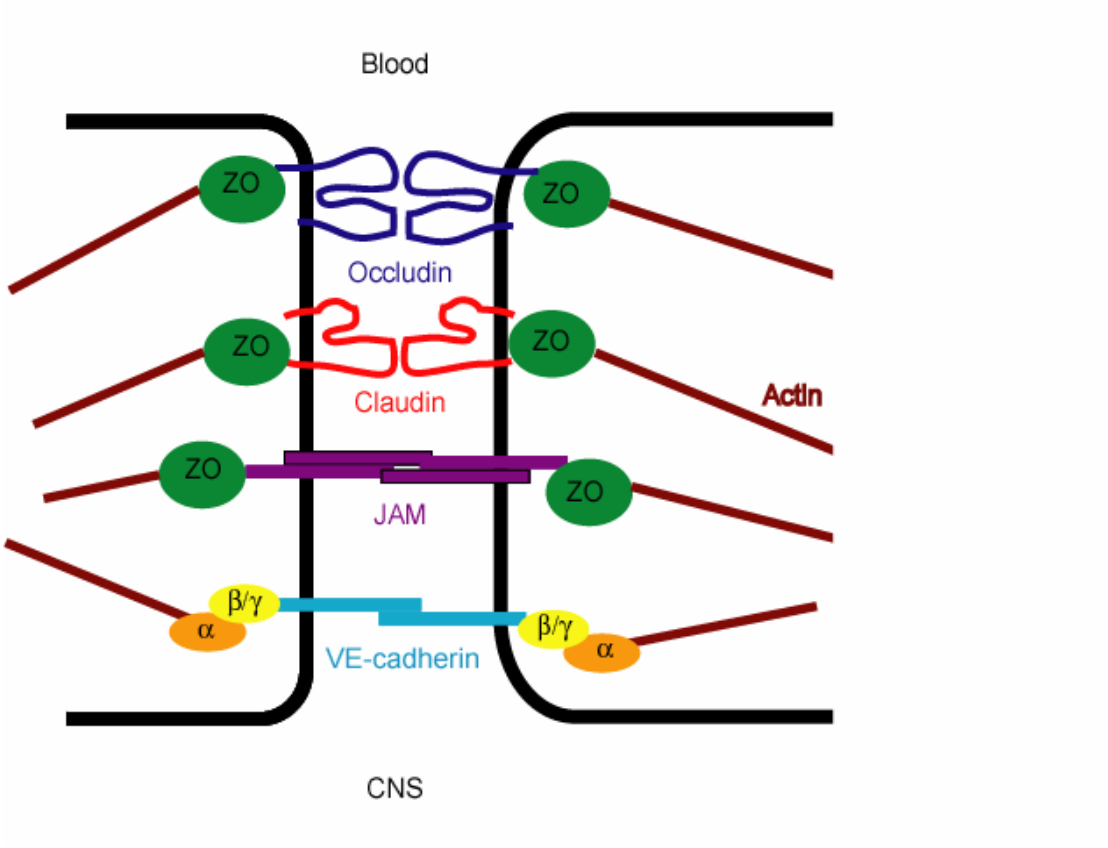


**Figure 1.2**. **Interendothelial Cleft.**
Diagram of endothelial junctions formed at the BBB. Zonula-occuldens (green) connect the tight junctions (occludin (navy blue), claudin (red), and JAM (purple)) to the actin cytoskeleton (brown). Adherens junction, VE-cadherin (sky blue), is linked to the actin cytoskeleton by α-catenin (orange) and β/γ– catenin (yellow).

barrier disruption (33). The claudin family is made up of 24 integral membrane proteins (3, 34). Like occludins, claudins show contiguous localization along the endothelial cell borders. In addition, alterations in claudin expression have also been associated with BBB disruption under disease states (35). Further, claudin 5 knockout animals show a size selective increase of paracellular permeability to small molecules (<800 kDa tracers) across the BBB, but not to larger molecules (36). JAMs mediate the early attachment of adjacent endothelial membranes, and are also believed to play a role in the formation and maintenance of barrier integrity. In addition, accessory proteins zonula-occuldens (ZO1, 2, 3) are a critical component of the tight junction complex and help to link the above mentioned tight junction proteins to the actin cytoskeleton (37-38). Indeed, several studies have reported that alteration of ZO-1 expression, and thus a disruption of the tight junction/cytoskeleton connection, promotes a loss of barrier integrity (39-42). Furthermore, the expression of additional junctional proteins, adherens junctions, helps to establish the integrity of the endothelial barrier. Vascular endothelial (VE)-cadherin is an adherens junction protein expressed in brain microvessel endothelial cells, which is linked to the actin cytoskeleton by catenins ($\alpha$, $\beta$, and $\gamma$) and seems to be important for the correct organization of tight junctions (43-45). In fact, recent work has revealed that expression of VE-cadherin promotes a higher expression of claudin 5 and induces tighter barrier permeability (46-47).

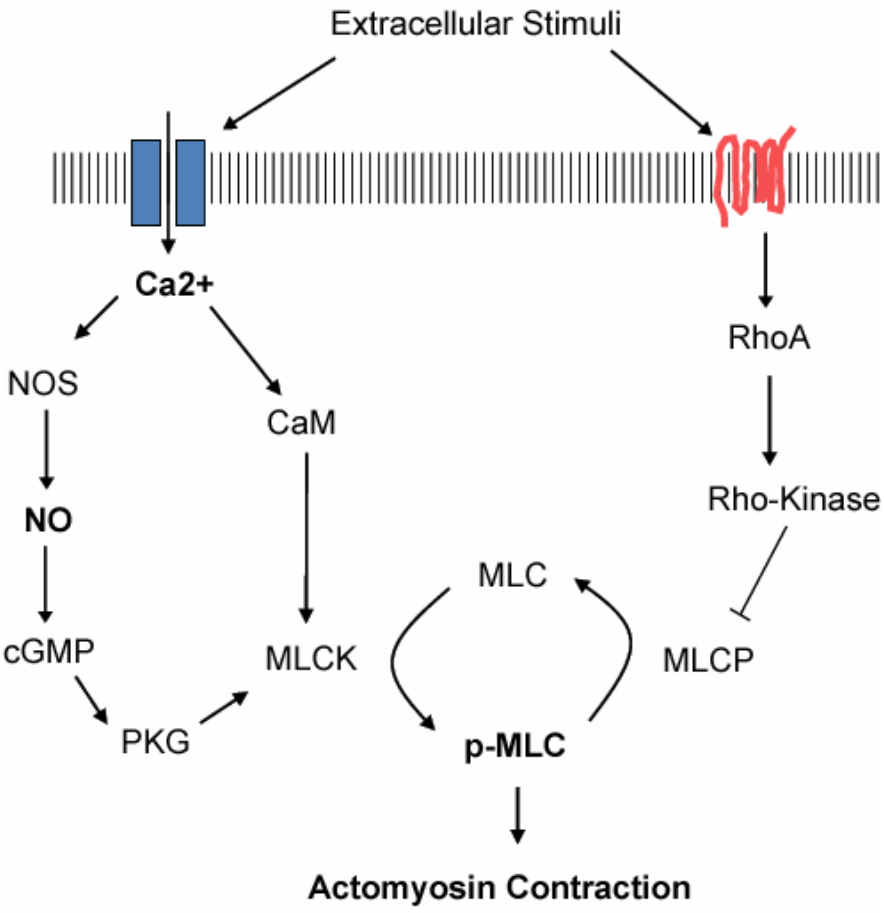


**Figure 1.3**. **Regulation of MLC.**
Diagram showing mechanisms which regulate MLC activity. MLC kinase (MLCK) activation, by NO-PKG or $Ca^{2+}$-CaM, leds to phosphorylation of MLC and initiation of actomyosin contraction. Conversly MLC phosphatase (MLCP), which may be inhibited by Rho kinase, reduces actomyosin contraction by dephosphorylating MLC.

## Cytoskeleton and Junctional Regulation

Recently, several studies have suggested a large role for the actin cytoskeleton in mediating the integrity of endothelial tight junctions. As such, experiments in which the actin cytoskeleton is disrupted are reported to lead to an increase in permeability across cell barriers, and barrier integrity restores once the actin cytoskeleton is allowed to reestablish (48-49). In addition, studies of brain microvessel endothelial cells have indicated a correlation between changes in paracellular permeability and alterations in expression of actin filaments (33). Although the mechanism by which the actin cytoskeleton modulates the cell junctions is currently unknown, it has been suggested that actin fibers may provide a necessary tension to enforce a close interlocking of junctions between apposing endothelial membranes (50-52). Actin-myosin contraction, leading to subsequent formation of actin stress fibers, has been reported as a component of endothelial barrier regulation (53-55). Phosphorylation of myosin light chain (MLC) serves as a trigger to initiate actin-myosin contraction, and is regulated by the activity of MLC kinase and MLC phosphatase (56). Indeed, MLC phosphorylation has been reported to increase during hypoxia-induced endothelial barrier disruption (57). Several factors have been identified to exert control over MLC phosphorylation, including regulation of MLC phosphatase (through Rho A induced inhibition) and MLC kinase (through intracellular calcium/nitric oxide (NO) dependent activation) (Figure 1.3).

NO is a diatomic gas which serves as an extracellular and intracellular secondary messenger molecule in many physiological mechanisms. In endothelial cells, NO is synthesized from L-arginine by endothelial nitric oxide synthase (eNOS), which can be activated by intracellular calcium (58-59). In addition to endothelial cell NOS expression, neurons and astrocytes express neuronal NOS, and inducible NOS is expressed in macrophages (60). Inducible NOS is considered to be a major component of NO synthesis under pathological conditions since immunological challenge promotes the induction of the inducible NOS gene. For instance, cytokines interleukin-1 and tumor necrosis factor alpha have been shown to promote inducible NOS expression (61). Further, subsequent to its synthesis, NO can interact with soluble guanylate cyclase (sGC) to catalyze the production of cyclic GMP (cGMP), and then mediate the activation of protein kinase G (PKG) (Figure 1.4). Of note, accumulating evidence points to a role for NO in mediating modulation of endothelial barrier permeability, likely through mechanisms involving MLC phosphorylation and actin-cytoskeleton modifications (56, 62-64).

In the cell, calcium ions also serve as important secondary messengers for intracellular signaling. Under physiological conditions, the cell maintains a low cytosolic calcium concentration ($[Ca^{2+}]i$) (≈100nM) in comparison to the extracellular calcium ion concentration (≈1-3mM). In order to accomplish this task the cell employs a series of ion pumps and exchangers to transport excess calcium ions out of the cell or into intracellular calcium stores, such as the

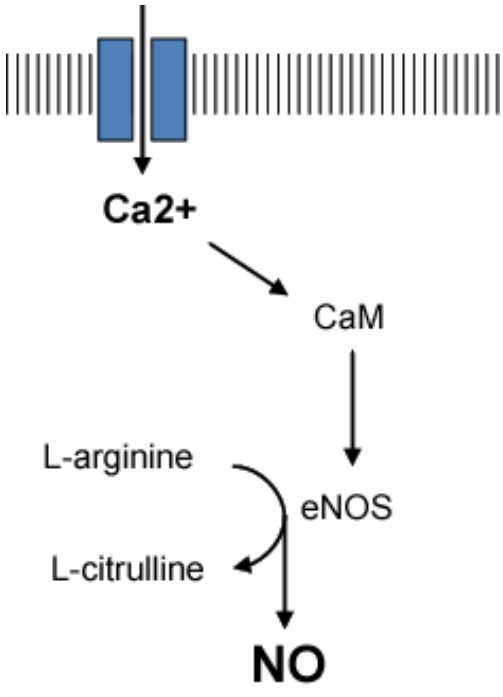


**Figure 1.4**. **NO synthesis.**
Diagram depicting calcium mediated NO synthesis. Activation of calmodulin (CaM) by $Ca^{2+}$ binding, may lead to CaM stimulation of endothelial nitric oxide synthase (eNOS). eNOS activation drives the conversion of L-arginine to NO and L-citrulline.

mitochondria and endoplasmic reticulum (Figure 1.5). In addition, a vast number of calcium permeable ion channels have been identified that contribute to the increases in intracellular calcium ions. Interestingly, multiple studies have shown that increased levels of $[Ca^{2+}]i$ can promote an increase of MLC kinase activity, which subsequently leads to actomyosin contraction (56, 65) (Figure 1.3). In fact, $[Ca^{2+}]i$ has been hinted to play an important role in the mechanism underlying loss of BBB integrity following induction of a hypoxic or hypertension injury (57, 66-68).

**Traumatic Brain Injury and BBB disruption**

Traumatic brain injury (TBI) is a detrimental condition which poses a worldwide health concern. It is referred to as the silent epidemic since its premier debilitations, memory and cognitive impairment, are difficult to identify. TBI is estimated to annually affect an average of 1.4 million individuals in the United States (69), and is rising as a top cause of mortality and financial burden. TBI is frequently diagnosed in victims of acts of violence, falls, and automotive collisions; it is believed to develop from mechanical injury sustained through physical impact or a rapid change in acceleration/deceleration to the brain. It has been demonstrated that following traumatic insult the brain tissue is launched into a series of rapid positional shifts, attributed to linear and rotational acceleration forces (70-71). In non-penetrating TBI, produced by rapid changes in acceleration, mechanical stress is believed to be the primary cause of injury

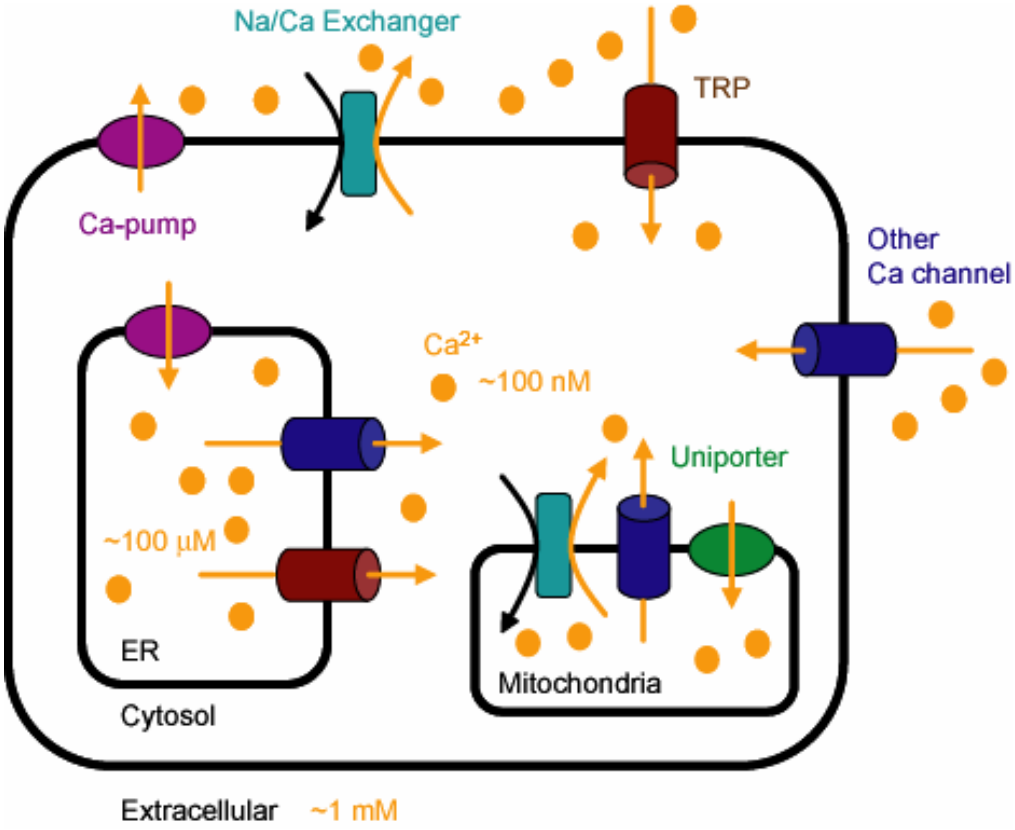


**Figure 1.5**. **Endothelial cell intracellular calcium dynamics.** Diagram depicting intracellular $Ca^{2+}$ mobilization. Calcium ions (gold) are shuttled into the cytosol by calcium-permeable ion channels (blue, brown) and exchangers (aqua). Conversely, calcium ions are shuttled out of the cytosol by $Ca^{2+}$ pumps (purple) and exchangers.

manifesting as shear stress and linear tension (stretching) on cells (72-73). Although the pathology is still largely unclear, TBI is generally considered to act in two phases: a primary injury immediately following mechanical insult (associated with axonal damage and necrosis at the site(s) of insult) and a secondary injury phase over the course of hours to months following the injury (typically encompassing tissue region outside the original site(s) of injury and associated with the development of secondary injury states) (74-77). As a result of traumatic insult, many clinical complications develop such as hypoxia, ischemia, edema, and blood brain barrier disruption. Interestingly, several studies have noted that following TBI cells undergo a rise of intracellular calcium (78-79). In fact, Fineman et. al. reported that cytosolic calcium may remain elevated for several hours following traumatic injury (80). Although it has been suggested that $[Ca^{2+}]i$ may be an important contributor to the TBI-induced BBB disruption, little is known about the calcium signaling events that ensue in brain microvessel endothelial cells following TBI.

**TRP channel Superfamily**

Transient receptor potential (TRP) proteins are a family of non-selective cation permeable channels, many of which are permeable to calcium ions (Figure 1.6). Since first being described in drosophila, TRP channels have been shown to be expressed in a multitude of animals and tissues (81-84). In mammals, the TRP channels expressed belong to 6 subfamilies: classical (TRPC1, 3-7),

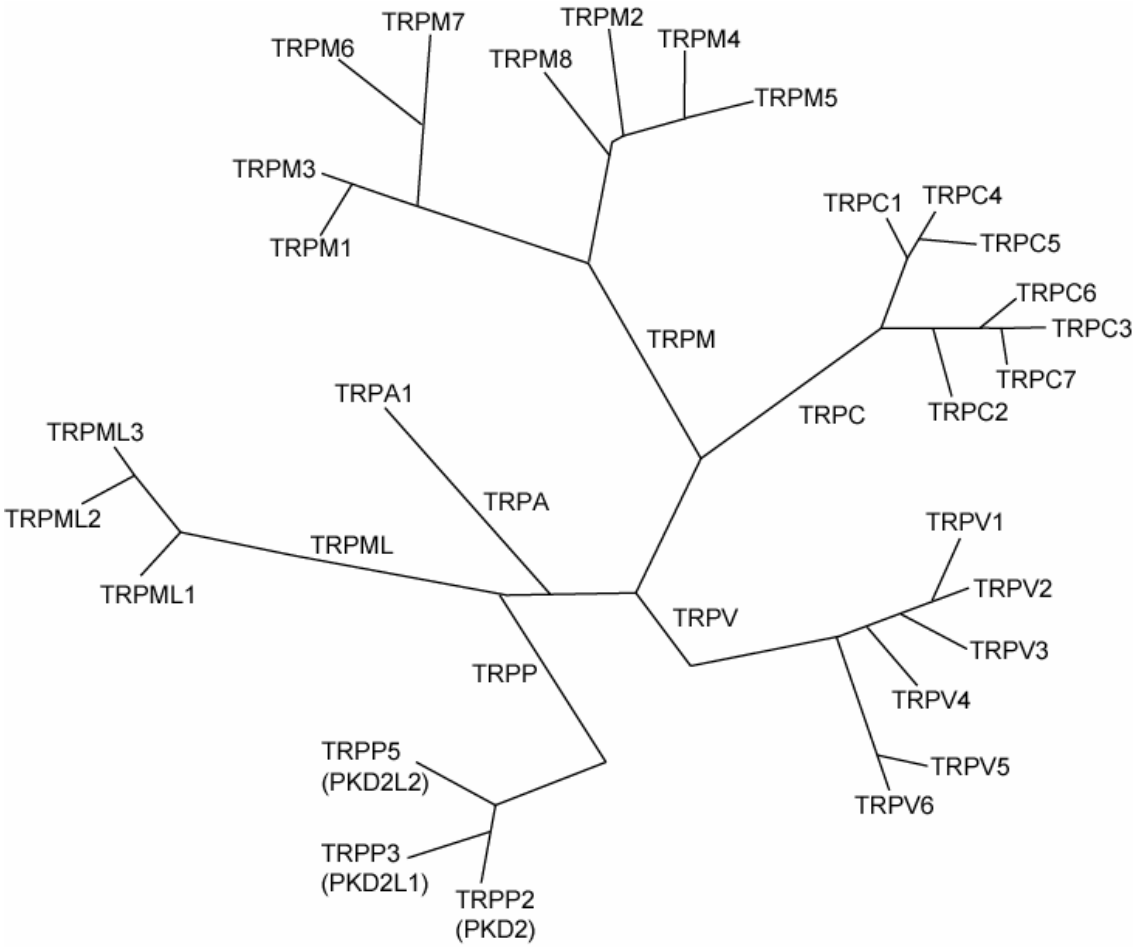


**Figure 1.6**. **TRP channel superfamily.**
Mammalian TRP superfamily phylogenic tree. Adapted from Christensen and Corey 2007, generated by aligning transmembrane domains of all TRP proteins.

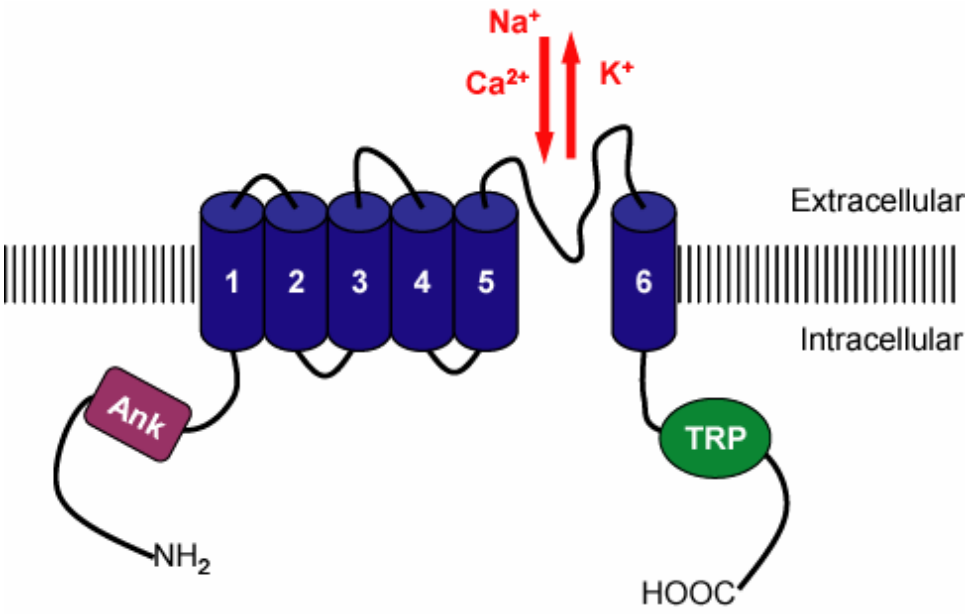


**Figure 1.7**. **TRP channel structure.**
Diagram depicting the generic TRP protein structure. The TRP isoform consists of six transmembrane domains (blue) protein with a putative pore loop (permeable to cations (red)) between the 5$^{th}$ and 6$^{th}$ transmembrane domain, and with cytosolic amino and carboxy termini. The TRP protein contains protein to protein interaction sites: for example ankyrin repeats (purple) and TRP box (green).

vanilloid (TRPV1-6), melastatin (TRPM1-8), polycystin (TRPP2, 3, 5), mucolipin (TRPML1-3), and ankyrin (TRPA1). In general, the TRP proteins structure consists of six transmembrane spanning domains with an ion conductive pore loop between the $5^{th}$ and $6^{th}$ transmembrane domain, and cytosolic carboxy and amino-termini with multiple protein-to-protein interaction sites (Figure 1.7). Functional channels are believed to be formed by a homo/heterotetramer configuration of TRP proteins. Particularly interesting is the ability of TRP channels to be activated by an impressive diversity of stimuli (such as changes in temperature, pH, and osmolarity, to name a few). This broad range of activation allows TRP channels to play a role in a plethora of diverse physiological functions. For instance, TRPM5 appears to serve as an important component in taste since TRPM5 knockout mice display a loss of sensitivity to sweet and bitter tastes (85). In addition, TRPV channels (V1, V3, and V4) seem to mediate an critical component of thermo-sensation since mice lacking these channels show an inability to discriminate between various temperature ranges (86-88). Further, TRPA1 channels have been proposed to play a role in auditory response during early development, as loss of channel expression reduced the response to sound (89-90). Hence, TRP channels are a unique family of ion channels which are involved in a multitude of physiological pathways.

**Mechanical sensation**

Mechanical stimuli, noted to be a major component of TBI, have been reported to induce functional modification of several proteins including g-protein coupled receptors and ion channels (91-93). TRP channels seem to be activated by a broad range of stimuli including mechanical stress (89, 94-96). The list of channels that are sensitive to mechanical stress includes proteins from multiple subfamilies. For example, TRPV4 has been reported to respond to mechano-stimuli delivered by hypotonic and shear stress (97-101). These studies proposed that TRPV4 is likely not activated directly by tension applied on the bilayer but rather through tethered and secondary biochemical signaling mechanisms occurring in response to osmomechanical stress. In addition, TRPP2 has been reported to mediate a mechanosensitive response to fluid flow in primary cilium of renal epithelium (102-104). Indeed TRPP2, which by its self has no mechano-sensitivity, seems to form a mechanosensitive complex when it is expressed with the mechano-sensor PKD1. Furthermore, TRPC1 was demonstrated to be activated by directly applying tension to the lipid bilayer (105). Through a series of patch-clamp experiments where cells expressing TRPC1 were exposed to negative pressure, it was suggested that the channel is likely gated through a bilayer-dependent mechanism.

As there appears to be no uniform mechanism of mechanical-induced activation, three potential mechanisms have been proposed to explain the activation of ion channels by mechanical stress (89, 94, 96) (Figure 1.8). 1) The bilayer-dependent mechanism, proposes that channels are activated by tension which bends or deforms the cell membrane causing membrane lipids to pull

away from the channel protein. As a result hydrophobic sites of the channel become exposed, increasing hydrophobic forces, which then promote conformational change of the channel and possible activation. 2) The tethered mechanism, supposes channels to be linked to accessory molecules, such as extracellular matrix proteins or cytoskeletal proteins, and as mechanical forces acting on these accessory molecules tension is then transmitted to the attached ion channel causing its activation in a lipid bilayer independent manner. 3) The mechano-biochemical conversion mechanism, suggests that channels may not be directly activated by mechanical forces, but rather channels may be activated through secondary signaling mechanisms initiated as a result of mechano-stimulus.

**TRP channels and barrier regulation**

Interestingly, TRP channels have been reported to regulate the function of endothelial barriers. In fact, TRPV (V4) and TRPC (C1 and C4) channels were demonstrated to modulate the integrity of alveolar-capillary barrier (106-107). Indeed, activation of TRPV4 was reported to mediate disruption of the alveolar-capillary barrier following acute lung injury (108). Of note, previous work in our lab has revealed the expression of several TRP channels in brain microvessel endothelial cells (67). Further, hypoxic studies on brain microvessel endothelial cells demonstrated that application of a nonspecific cation channel inhibitor, SKF96365 (known to inhibit TRPC channels), helped reduce barrier permeability

after insult (57). These findings have led our laboratory to investigate the role that TRP channels may play following exposure of brain endothelial cells to TBI-like mechanical stress. Our goal was to identify a potential mechanism to explain the phenomenon of mechanical stress induced endothelial barrier disruption, in hopes of obtaining a better understanding of the effect of mechanical stress on the BBB that may lead to future therapeutic strategies for TBI patients.

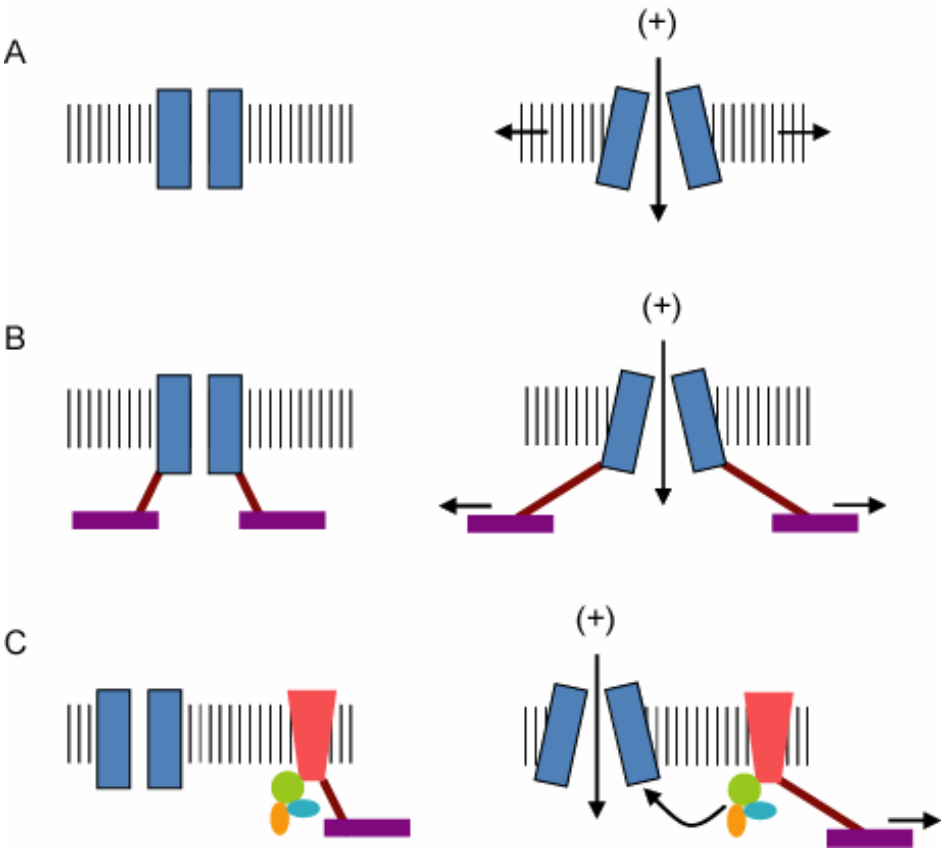


**Figure 1.8**. **Mechanisms of mechano-sensation.**
Diagram showing potential gating mechanisms for mechano-sensitive ion channels. **A.** bilayer-dependent model supposes that tension on the bilipid membrane causes exposure of hydrophobic mismatches favoring channel opening. **B.** tethered model suggests that channel opening is due to tension on accessory proteins inducing conformational change of the ion channel. **C.** mechano-biochemical conversion model supposes that channel opening is not directly mediated by tension but rather by secondary signaling initiated following mechanical stimuli.

# Chapter Two: Mechanical stretch triggers an increase of intracellular calcium in brain endothelial cells

## Background

TBI is believed to develop from mechanical injury brought on by physical impact or a rapid change in acceleration/deceleration of the head (75, 109). Following traumatic insult the brain undergoes a series of rapid positional shifts in varying direction, which are attributed to linear and rotational acceleration forces (72, 74, 76). Rotational forces are proposed to manifest as shear stress and linear tension (stretching) on the brain tissue, leading to the initiation of complex cellular signaling mechanisms. Although much is unclear as to how mechanical stress triggers the destructive signaling pathways in TBI, it is evident that mechanical stimuli are able to induce functional modification of many proteins including ion channels (89, 95).

Three potential mechanisms have been proposed to explain the activation of ion channels by mechanical stress (89, 94) (Figure 1.8). 1) The bilayer-dependent mechanism, proposes that channels are activated by tension which bends or deforms the cell membrane causing membrane lipids to pull away from the channel protein. As a result hydrophobic sites of the channel become exposed, increasing hydrophobic forces, which then promote conformational change of the channel and possible activation. 2) The tethered mechanism, supposes channels to be linked to accessory molecules, such as extracellular matrix proteins or cytoskeletal proteins, and as mechanical forces acting on these accessory molecules tension is then transmitted to the attached ion channel causing its activation in a lipid bilayer independent manner. 3) The

mechano-biochemical conversion mechanism, suggests that channels may not be directly activated by mechanical forces, but rather channels may be activated through secondary signaling mechanisms initiated as a result of mechano-stimulus.

In cells, calcium ions serve as important second messengers of intracellular signaling, and play a role in many essential physiological mechanisms. Endothelial cells express an array of proteins to transport calcium ions either in or out of the cell and in or out of the intracellular calcium stores (110-111). The endoplasmic reticulum and mitochondria serve as intracellular storage sites for $Ca^{2+}$. Several TBI studies have reported a rise of $[Ca^{2+}]i$ following injury in neurons, glia, and endothelial cells (78-80). Thus, it seems likely that mechano-sensitive proteins, ion channels, may be expressed on these cells and directly contributing to the observed $[Ca^{2+}]i$ increase.

## Methods

### Cell Culture & Solutions

The mouse brain microvessel endothelial cells (bEnd3 cells) were used for all studies (American Type Culture Collection). The bEnd3 cells are an immortalized cell line originally generated by Montesano et. al. in 1990 (112). The bEnd3 cells were used as a model of BBB since previous studies had revealed that the bEnd3 cells retained several critical components of the in vivo barrier. These components included restricted permeability to molecules (< 650 mw) and expression of tight junction proteins occludin, claudin 1, claudin 3, claudin 5, ZO-1, and ZO-2 (113). In addition, early experiments using primary culture mouse brain microvessel endothelial cells demonstrated that the response to mechanical stretch (induced by use of the cell injury controller device, see below) was similar in both primary culture cells and bEnd3 cells (unpublished data).

Cells were grown in DMEM culture media with 3.7 g/L sodium bicarbonate, 4 mmol/L glutamine, 4.5 g/L glucose, 100 μg/ml penicillin, 100 μg/ml streptomycin, and 10% FBS. During growth, cells were kept in a humidified incubator at 37°C with 10% $CO_2$ - 90% room air, and grown to confluence over 4-5 days. For experiments cells were seeded at a density of 0.14-0.6 x $10^5/cm^2$ on collagen coated BioFlex elastic membrane supports (Flexcell International Corp) or glass cover slips. During intracellular calcium measurements, cells were studied in a isotonic modified balanced salt solution (MBSS) containing (in

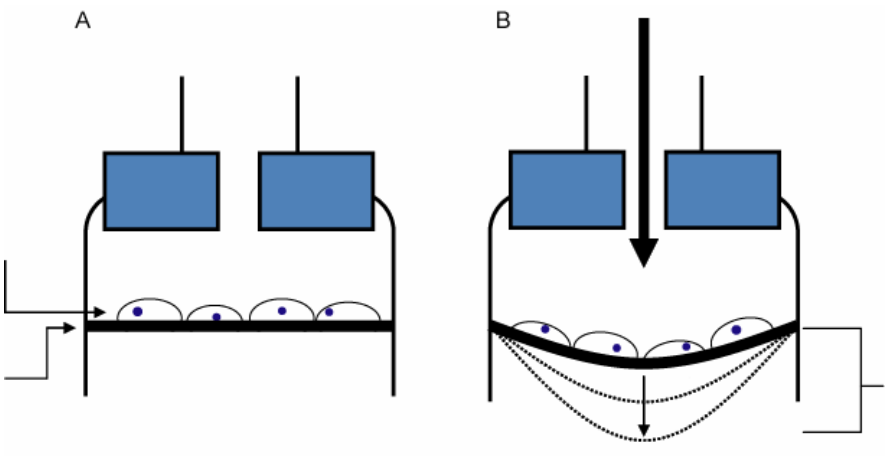


**Figure 2.1**. **Cell Injury Controller II.**
**A.** Brain microvessel endothelial cells are grown on an elastic membrane. **B.** Mechanical stretch is applied by a short (50 ms) injection of nitrogen gas, which deforms the elastic membrane.

mmol/L): 140 NaCl, 5.4 KCl, 2 $CaCl_2$, 0.5 $MgCl_2$, 0.4 $MgSO_4$, 3.3 $NaHCO_3$, 10 HEPES, 5.5 glucose, and pH of 7.4. A calcium-free MBSS solution was also utilized containing 1 mmol/L EGTA in place of 2 mmol/L $CaCl_2$.

**Mechanical Cell Injury**

In preparation for injury, cells were grown to confluence on BioFlex 6-well culture plates with collagen coated silastic membranes (Flexcell International Corp). Biaxial stretch was applied on cell cultures using the Cell Injury Controller II system (CIC II, Virginia Commonwealth University) (Figure 2.1). The device delivered a 50 ms burst of nitrogen gas, which produces a downward deformation of the elastic membrane and adherent cells. During membrane deformation, pressure recorded inside the well ranged from 1.8 - 4.5 psi. Elastic membranes were stretched to an increased membrane diameter of 20% (5.5mm), 35% (6.5 mm), and 55% (7.5 mm) (114-115). These degrees of stretch are believed to be similar to the mechanical stress range exerted on human brain during rotational acceleration-deceleration injury (114, 116-117). Mechanical stretch above 35% leads to cell damage and apoptosis (in neurons and astrocytes) of similar proportion as observed for in vivo TBI. Further, the CIC II is capable of delivering a strain of 0.1-0.6, which encompasses strain ranges estimated for TBI (strain threshold for concussion and axonal injury is estimated to be 0.5-0.3) (72, 117).

**Calcium imaging**

Measurement of cytosolic calcium concentration was accomplished with the use of the Fura-2AM fluorescent indicator (67, 101). Cells were seeded on BioFlex 6-well plates and incubated with 5 μmol/L Fura-2AM (Calbiochem) at room temperature for 1 hour in the dark. Following incubation cells were washed with MBSS solution in preparation for imaging. The BioFlex plates were affixed to the microscope stage of an InCyt Im Imaging workstation (Intracellular Imaging, Inc) and imaged with a Nikon Eclipse TS 100 inverted microscope using a 20X super fluor objective (NA = 0.75) and a 12-bit CCD camera (Pixel Fly, Cooke). Cells loaded with Fura-2 were excited alternately with 340 and 380 nm illumination and the fluorescence emission images at 510 nm ratioed as an index of intracellular calcium. The ratios were converted to a $[Ca^{2+}]i$ value using the equation: $[Ca^{2+}]i = K_d\beta(R-Rmin)/(Rmax-R)$ (118), where $K_d$ is the $Ca^{2+}$ dissociation constant of fura 2, $\beta$ is the ratio of the fluorescence emission intensity at 380 nm excitation in $Ca^{2+}$-depleting and $Ca^{2+}$-saturating conditions, R is the ratio at any time, Rmin is the minimum ratio in $Ca^{2+}$-depleting conditions (addition of 5 μmol/L EGTA and 2 μmol/L ionomycin), and Rmax is the maximum ratio in $Ca^{2+}$-saturating conditions (2 μmol/L ionomycin plus 10 mM $Ca^{2+}$). For each experiment, 10-30 cells were simultaneously monitored and their fluorescence emission ratios were averaged at the end of recording.

**Statistical Analysis**

Data was calculated as mean ± SE. One-way ANOVA and/or student t-test, performed with Sigma Stat, was used to compare the difference among

groups. n is representative of the number of experiments conducted; for Fura-2 and DAF-FM experiments an n of 1 is representative of average response from 15-30 cells. Statistical significance ( * ) was determined as $p < 0.05$, (**) depicts $p < 0.001$.

## Results

### Mechanical stretch-induced $[Ca^{2+}]i$ dynamic

Previous work on astrocytes and neurons had revealed that exposure to mechanical stretch resulted in a prolonged state of increased $[Ca^{2+}]i$ (114-115). To investigate the signaling response of brain endothelial cells exposed to mechanical stretch the Cell Injury Controller II unit (Virginia Commonwealth University) was utilized to produce a TBI-mimicking rapid-stretch injury (114, 116) (Figure 2.1). Rapid delivery of a nitrogen gas pulse (50 ms duration), led to deformation of the elasticized membrane to which the cells were attached (magnitude of membrane deformation was controlled through regulation of gas pressure). Application of membrane stretch below 10% failed to induce a change in intracellular calcium while higher levels of stretch induced an increase in $[Ca^{2+}]i$, demonstrating a threshold for initiation of the stretch-induced $[Ca^{2+}]i$ dynamic in bEnd3 cells (Figure 2.2). In a typical cell the peak $[Ca^{2+}]i$ response was measured at one minute post-stretch (the earliest time point at which cells could be re-imaged for measurement of $[Ca^{2+}]i$ after stretch). Following the peak was a progressive decline in $[Ca^{2+}]i$, over the next 2-3 minutes, until the establishment of a pseudo-plateau, a long lasting high $[Ca^{2+}]i$ state (persisting for greater then 60 minutes in our recordings). One minute after application of the stretch yielded a $[Ca^{2+}]i$ increase of 96 ± 22 nM (n = 13) with 20% stretch, 198 ± 27 nM (n = 12) with 35% stretch, and 219 ± 21 nM (n = 12) with 55% stretch (Figure 2.2).

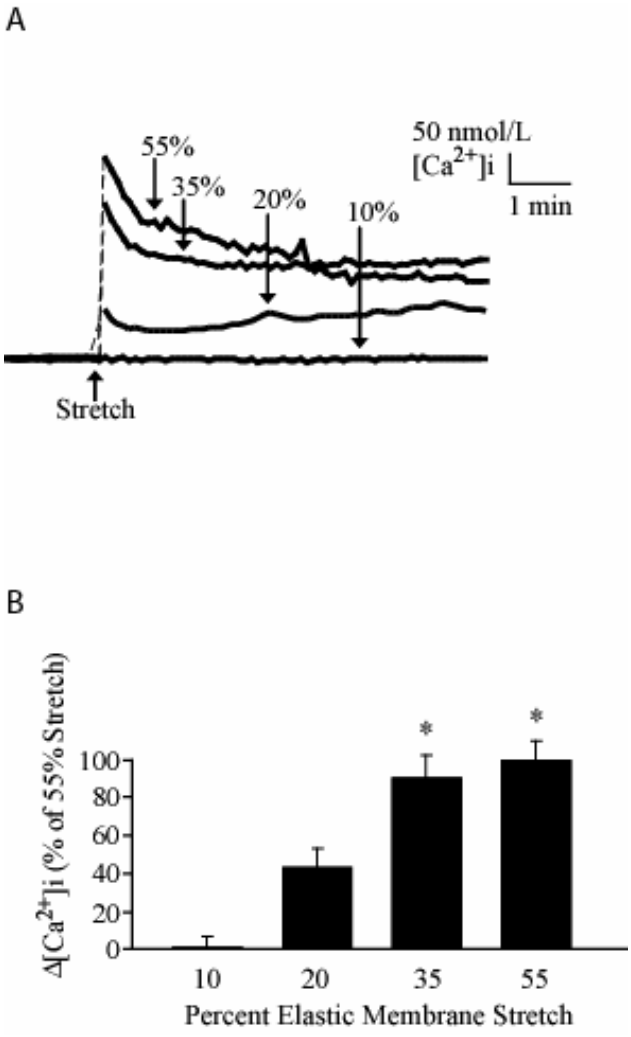


**Figure 2.2**. **Stretch magnitude dependent $[Ca^{2+}]i$ response.** **A.** Representative traces of $[Ca^{2+}]i$ following application of elastic membrane stretch (10, 20, 35, and 55%). **B.** Average $[Ca^{2+}]i$ increase 1 min post-stretch produced by varying degrees of stretch of 10 (n = 2), 20 (n = 13), 35 (n = 12), and 55% (n = 12) (* $P < 0.05$ vs 10% stretch, ANOVA Tukey test). Dashed lines in traces represents gap in imaging acquisition. Taken with permission from publisher from (4).

**Stretch-induced extracellular $Ca^{2+}$-influx**

In order to better characterize the stretch-induced $[Ca^{2+}]i$ dynamic it was critical that the source(s) of $Ca^{2+}$, which flood the cytosol following stretch application, be identified. Since previous studies had suggested that extracellular calcium influx was largely responsible for the establishment of high $[Ca^{2+}]i$ conditions following neuronal injury, we assessed the possibility of extracellular calcium being important for the development of the stretch-induced dynamic (80, 115). To investigate the contribution of extracellular calcium influx to the stretch-induced $[Ca^{2+}]i$ increase, stretch was applied under conditions in which extracellular calcium was removed. In the absence of extracellular calcium, a rapid 35%-stretch stimulus led to a transient, increase in $[Ca^{2+}]i$, with a peak response of 84 ± 17 nM (n = 5) (Figure 2.3A-B). This peak $[Ca^{2+}]i$ increase was significantly lower than the observed control response, 198 ± 27 nM (n = 12). We also observed, in the absence of extracellular calcium, that the peak was followed by a decline back to the initial baseline (-8 ± 2 nM, n = 5) (Figure 2.3A, C). This was also significantly different from the response seen in control where the $[Ca^{2+}]i$ is held at a higher pseudo-plateau (118 ± 17 nM, n = 12); demonstrating that the majority of the stretch-induced $[Ca^{2+}]i$ dynamic was mediated through extracellular calcium influx.

**Stretch-induced $Ca^{2+}$ release from intracellular stores**

To further elucidate the stretch-induced $[Ca^{2+}]i$ response, the role of calcium release from intracellular stores was examined. Treatment of cells with

thapsigargin (TG), a $Ca^{2+}$-ATpase pump inhibitor, was used as a means to deplete the endoplasmic reticulum calcium store. We observed that the 35% stretch-induced $[Ca^{2+}]i$ dynamic was largely unaffected by depletion of the intracellular stores as prior treatment with TG led to a stretch-induced increase of 225 ± 50 nM (n = 4) (comparable to the response seen in control conditions, 206 ± 24 nM, n = 15) (Figure 2.4A-C). Further, under conditions of zero extracellular calcium, the stretch-induced transient $[Ca^{2+}]i$ response (peak of 84 ± 17 nM, n = 5) was abolished if the internal stores were first depleted with TG (peak of -7 ± 22 nM, n = 3) (Figure 2.4D). Hence, exposure of brain endothelial cells to mechanical stretch produced a $[Ca^{2+}]i$ increase, resulting from a prolonged extracellular calcium influx and a transient calcium release from intracellular stores.

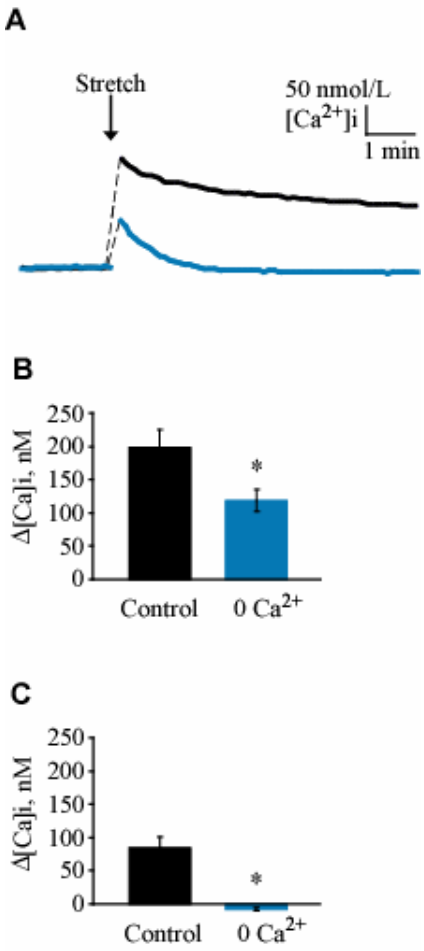


**Figure 2.3. 35% stretch-induced extracellular $Ca^{2+}$ influx.**
**A.** 35% stretch induces a rise of $[Ca^{2+}]i$ under control conditions with 2mM extracellular $[Ca^{2+}]$ (black trace), but is greatly reduced with zero extracellular $[Ca^{2+}]$ (blue trace). **B.** Average $[Ca^{2+}]i$ increase 1 min post-stretch (control n = 12, zero Ca n = 5). **C.** Average $[Ca^{2+}]i$ increase 5 min post-stretch (control n = 12, zero Ca n = 5). * $P < 0.01$, t-test. Dashed line in traces represents gap in imaging acquisition. Taken with permission from publisher from (4).

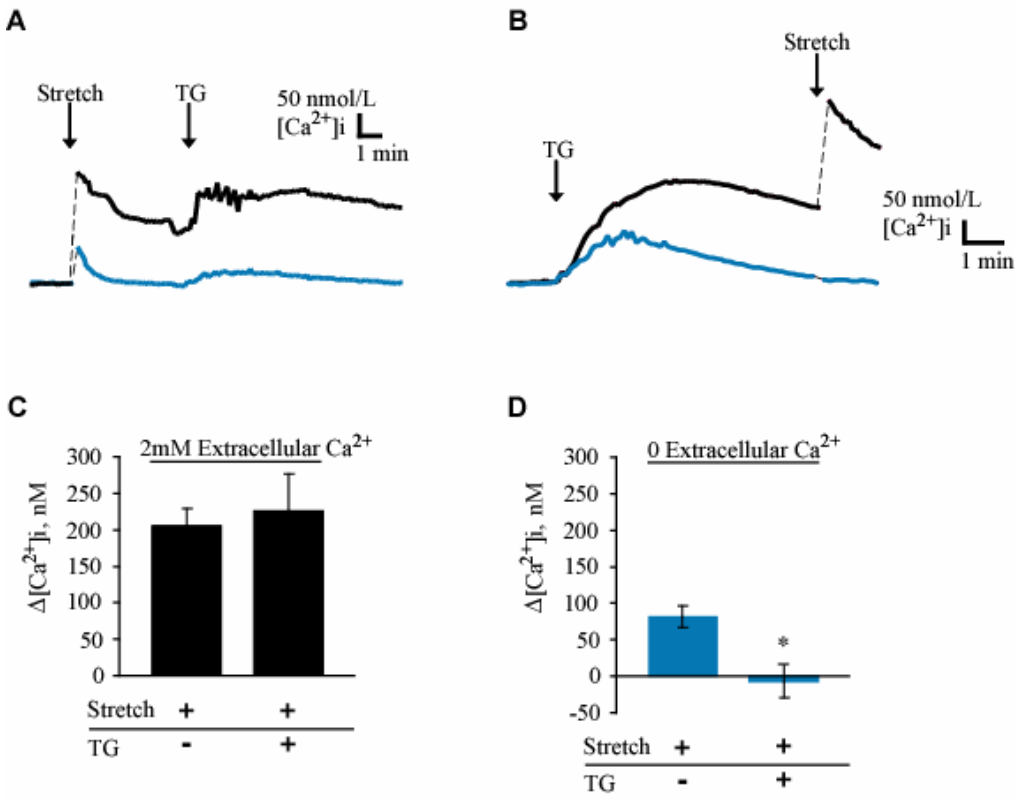


**Figure 2.4. 35% stretch-induced $Ca^{2+}$ release from intracellular stores.** **A.** 35% stretch application prior to 10 μmol/L TG treatment, under conditions with 2mM extracellular [$Ca^{2+}$] (black trace) or zero extracellular [$Ca^{2+}$] (blue trace). **B.** TG-mediated (10 μmol/L ) depletion of intracellular calcium stores followed by stretch application, same extracellular [$Ca^{2+}$] conditions as (A). **C.** Summary graph of stretch-induced [$Ca^{2+}$]i increase (1 min post-stretch) with or without TG-mediated intracellular store depletion in the presence of 2mM extracellular [$Ca^{2+}$]. **D.** Stretch-induced [$Ca^{2+}$]i increase (1 min post-stretch) with or without TG-treatment in the presence of zero extracellular [$Ca^{2+}$] (* $P < 0.05$, t-test, control n = 3-8). Dashed line in traces represents gap in imaging acquisition. Taken with permission from publisher from (4).

# Chapter Three: TRP channels mediate calcium signaling after mechanical stretch

## Background

Transient receptor potential channels are among the ion channel families reported to be expressed by brain microvessel endothelial cells. TRP channel proteins are a family of non-selective cation permeable channels, many of which are permeable to calcium ions (81-83, 119). Since first being described in drosophila as a light sensitive channel, TRP channels have been identified to express in a multitude of species and tissues (84). In mammals, TRP proteins are divided into 6 subfamilies: classical (TRPC1-7), vanilloid (TRPV1-6), melastatin (TRPM1-8), polycystin (TRPP1-4), mucolipin (TRPML1-3), and ankyrin (TRPA1). Of particular interest among these channels is their sensitivity to a broad range of stimuli including mechanical stress. TRPC1 for example, has been reported to be activated when stretch tension is directly applied to the lipid bilayer (105). In addition TRPP2, is described to form a mechanosensitive complex with polycystin kidney disease 1 responsive to shear stress (103).

Further, several studies have suggested that TRP channels may play an important role in regulation of permeability across endothelial cell barriers. Indeed, experiments looking at the effect of hypoxic stress on BBB permeability demonstrated that application of non-selective cation channel inhibitor, SKF96365, helped reduce barrier permeability after insult (68). In addition, TRP channels (TRPV4, TRPC4, TRPC6) are implicated in the regulation of the lung endothelial barrier, where activation of these TRP channels mediates an increase of permeability across the barrier (106-108, 120). Further, studies in our lab have

hinted that TRPC channels may play a critical role in mediating hypoxia-induced endothelial barrier disruption as application of SKF96365, a non-selective TRP channel inhibitor, alleviated the effect of hypoxic insult (57). Thus, TRP channels may play a significant role in the mechanisms regulating endothelial barrier integrity under other injury states, such as following TBI-mechanical insult.

## Methods

See Chapter 2 methods section for methodology regarding Cell Culture & Solutions, Mechanical Cell Injury, Calcium imaging, and Statistical Analysis.

### RNA collection & RT-PCR

Total RNA extraction from cells was accomplished using TRIzol reagent (Invitrogen). Expression of TRP channels was examined using SuperScript One-Step RT-PCR Platinum Taq (Invitrogen). Primer sets for TRP channels were obtained from Sigma-Alrich. PCR primer sequences are listed in table 3.1. In these experiments, 0.5-1 μg sample RNA were reverse transcribed and amplified using Taq polymerase. The RT-PCR reactions were run with use of the GeneAmp PCR system 2400 (Perkin Elmer). PCR products were separated on 1% agarose gels, stained with ethilium bromide, and photographed with the ChemiGenius bioimaging system (Syngene). GAPDH was used as a standard loading control.

### Immunoblotting

Protein was harvested by washing the cells with PBS, then scraping cells off culture plates and treating with RIPA cell lysis buffer with protease inhibitor (Sigma). For western blots, 20-30 μg of sample protein were run in 4-20% SDS-PAGE gradient gel, then transferred to PVDF membrane, and blocked with 5%

| | Forward Primer | Reverse Primer | Size (bp) |
|---|---|---|---|
| TRPV2 | tga tga agg ctg tgc tga ac | cag agc atg cag gac tgt gt | 398 |
| TRPV4 | atc aac tcg ccc ttc aga ga | ggt gtt ctc tcg ggt gtt gt | 339 |
| TRPC1 | gta ccc gag cac gga cct | aac agc att tct ccc aag ca | 250 |
| TRPC4 | gct gga gga gaa gac act gg | gac ctg tcg atg tgc tga ga | 211 |
| TRPC6 | caa tcg cgg tgg ttt taa gt | cgc atc atc ctc aat ttc ct | 416 |
| TRPM2 | cag agc aaa cga agg aaa gg | tca gta acg cct gca gaa tg | 387 |
| TRPM4 | gag agg atc atg acc cga aa | gtc att cag cag agc atc ca | 255 |
| TRPM7 | gct cca tgg gga gtg ata ga | atc aaa gcc acc aca gga ac | 254 |
| TRPA1 | gcg gag act tgg aca tga tt | tgg aga gcg tcc ttc aga at | 290 |
| TRPP1 | tct tca agc tct cgc tga ca | gga cac aag gac ggt caa gt | 353 |
| TRPP2 | ggt ggt ggc aaa ctg aac tt | tct cca gct tga caa tca cg | 412 |

**Table 3.1. TRP channel pcr-primer sequences.**
Taken with permission from publisher from (4).

milk for 1-2 hr. Subsequently, membranes were incubated with anti-TRPP2 (1:200, Santa Cruz Biotechnology) or TRPC1 (1:200, Santa Cruz Biotechnology) overnight at 4˚C. Following washing, membranes were incubated with anti-rabbit secondary antibody (1:500-1:5000). Beta-actin and alpha-tubulin were used as an internal loading control.

**RNA Interference**

For knockdown of TRP channel protein expression, siRNA targeting TRPC1 (Santa Cruz Biotechnology) and TRPP2 (SeqWright) were utilized. TRPC1 siRNA was constructed with use of Silencer siRNA construction kit (Ambion). Cells were transfected with use of siPORT Amine reagents (Ambion) and 20-30 nmol/L target siRNA. Cells were plated at a density of approximately 0.14-0.6 x $10^5/cm^2$ either on glass cover slips or silastic membranes (coated with collagen IV). After 18-24 hours, cells were transfected with a mixture of siPORT$^{TM}$ Amine transfection reagent and the appropriate siRNA complex. Cells were then allowed to incubate for 24-72 hours at 37$^o$C, and subsequently employed for appropriate assay. Scrambled siRNA (Santa Cruz Biotechnology) was used as a transfection control.

## Results

### TRP channel expression on bEnd3 cells

Given the many reports addressing the mechano-sensitivity of TRP channels (94, 96, 121), and the recent reports involving TRP channels in the control of endothelial barrier permeability (57, 106-107), I assessed the role TRP channels play in the brain endothelial cell response to mechanical stress. To determine the potential involvement of TRP channels in mediating the stretch-induced $[Ca^{2+}]i$ response, I first assessed the expression of TRP channels in bEnd3 cells. Semi-quantitative RT-PCR analysis was used to elucidate the mRNA expression of TRP channels in bEnd3 cells. TRP channel isoforms from the vanilloid (V2, V4), canonical (C1, C4, C6), melastatin (M2, M4, M7), and polycystin (P2) subfamilies were found to be expressed (Figure 3.1).

### Role of TRP channels in the stretch-induced $[Ca^{2+}]i$ dynamic

As multiple TRP channels are expressed in bEnd3 cells, pharmacological inhibitors were used to systematically determine which TRP isoforms play a role in the stretch-induced $[Ca^{2+}]i$ response. Treatment of cells with 10 μM SK&F96365, a non-selective cation channel blocker that has been used as a TRPC channel inhibitor, after stretch led to a reduction of 66% ± 19 % (n = 4) from control $[Ca^{2+}]i$ response (Figure 3.2A, D). Similarly, application of 10 μM LOE908, a non-selective cation channel blocker that has been used as a

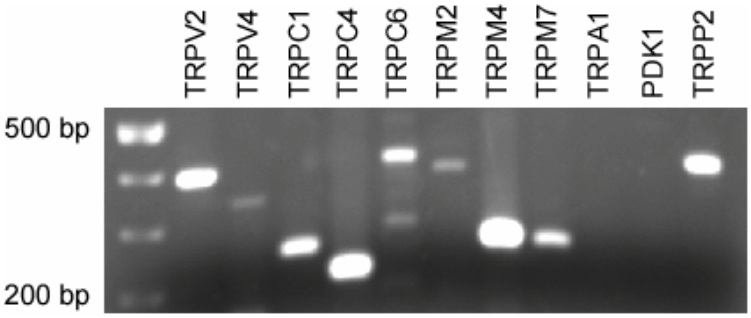


**Figure 3.1. TRP channel mRNA expression.**
RT-PCR showing mRNA expression for a wide range of TRP channels on bEnd3 cells. Taken with permission from publisher from (4).

TRPC channel inhibitor, reduced the stretch-induced $[Ca^{2+}]i$ increase by 65% ± 16 % (n = 6) (Figure 3.2B, D). Thus, these data suggest that TRPC channels become activated following mechanical stretch and mediate a portion of the observed $[Ca^{2+}]i$ increase. Further, treatment with 10 μM amiloride, , a non-selective drug known to inhibit TRPP2 channels (as well as some $Na^+$ channels and the $Na^+/H^+$ exchanger), effectively diminished the stretch-induced $[Ca^{2+}]i$ increase by 86% ± 27% (n = 6) (Figure 3.2C, D). Hence, these results implicate TRPP2 channels as a potential contributor to the stretch-induced $[Ca^{2+}]i$ dynamic. Application of TRPV channel antagonist, 1 μM ruthenium red, failed to produce an inhibition of the stretch-induced $[Ca^{2+}]i$ increase (Figure 3.2D). Thus, it became apparent that TRPC and TRPP channels may mediate the stretch-induced calcium influx.

**TRPC1 and TRPP2 mediate the stretch-induced response**

Because of the lack of selectivity of the pharmacological inhibitors available to target the specific TRP channels subtypes, further approaches were used to identify the importance of individual channels. RNA interference, siRNA gene silencing, was used to specifically target TRP isoforms, allowing knockdown of the individual TRP channel protein expression. Reduction of protein expression after treatment with siRNA was assessed with western blots (Figure 3.3A). As a control cells were transfected with scrambled RNA, a sequence not specific to any protein mRNA. Cells treated with scrambled RNA showed stretch-induced $[Ca^{2+}]i$ response of 224 ± 30 nM, (at one minute post-

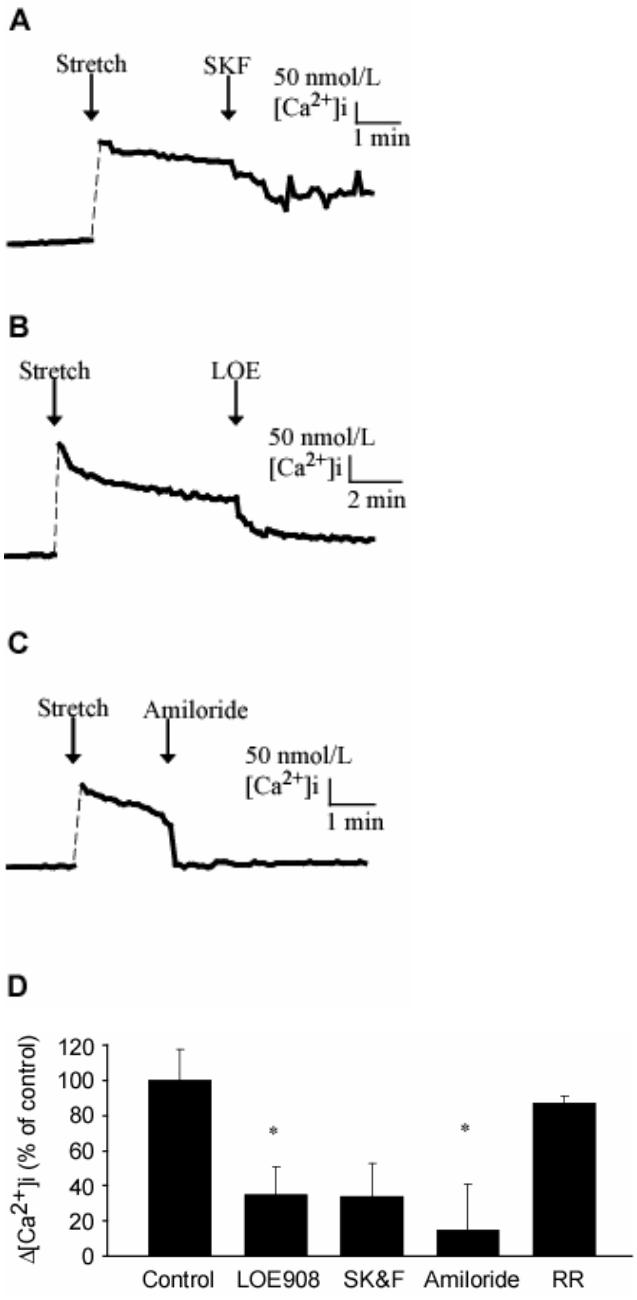


**Figure 3.2. TRP channels mediate stretch-induced $[Ca^{2+}]i$ response.**
Application of 35% stretch followed by treatment with **A.** TRPC inhibitor, SKF96365 (10 μmol/L, n = 4), **B.** TRPC inhibitor, LOE908 (10μmol/L, n = 6), and **C.** TRPP2 inhibitor, amiloride (10μmol/L, n = 6). Dashed line in traces represents gap in imaging acquisition. **D.** Summary bar graph of [Ca]i measurements after inhibitor application, normalized to the value of the control group. Results are expressed as mean ± SEM, t-test, * $P < 0.05$ vs control. Taken with permission from publisher from (4).

stretch, n = 6), which was similar to the response seen with non-transfected cells (Figure 3.3B-C, black bar). Knockdown of TRPC1 protein expression led to a stretch induced $[Ca^{2+}]i$ response with a modest decline one minute post stretch, 186 ± 19 nM (n = 6) (time point was chosen to represent peak response observed) (Figure 3.3C, red bar). At seven minutes post-stretch (time point chosen to represent established pseudo-baseline) TRPC1 knockdown led to a significant decline of the $[Ca^{2+}]i$ response, 84 ± 13 nM (n = 6) (scramble control value was 149 ± 40 nM, n = 5) (Figure 3.3D, red bar). In addition, knockdown of TRPP2 led to a significant decrease of the $[Ca^{2+}]i$ response one minute after stretch, 113 ± 22 nM (n = 7) (Figure 3.3C, blue bar), while at seven minutes post-stretch the stretch-induced $[Ca^{2+}]i$ showed a reduction to 89 ± 6 nmol/L (n = 3) (Figure 3.3D, blue bar). Further, when expression of both TRPC1 and TRPP2 were suppressed simultaneously the stretch-induced $[Ca^{2+}]i$ response was significantly decreased throughout the length of recording (measuring a value of 102 ± 14 nmol/L (n = 5) one minute post-stretch and 43 ± 7 nmol/L (n = 5) seven minutes after stretch) (Figure 3.3B-D, purple bar). Thus, these findings together suggest that TRPP2 and TRPC1 channels are activated following TBI-like mechanical stress and subsequently mediate the majority of the stretch-induced $[Ca^{2+}]i$ increase.

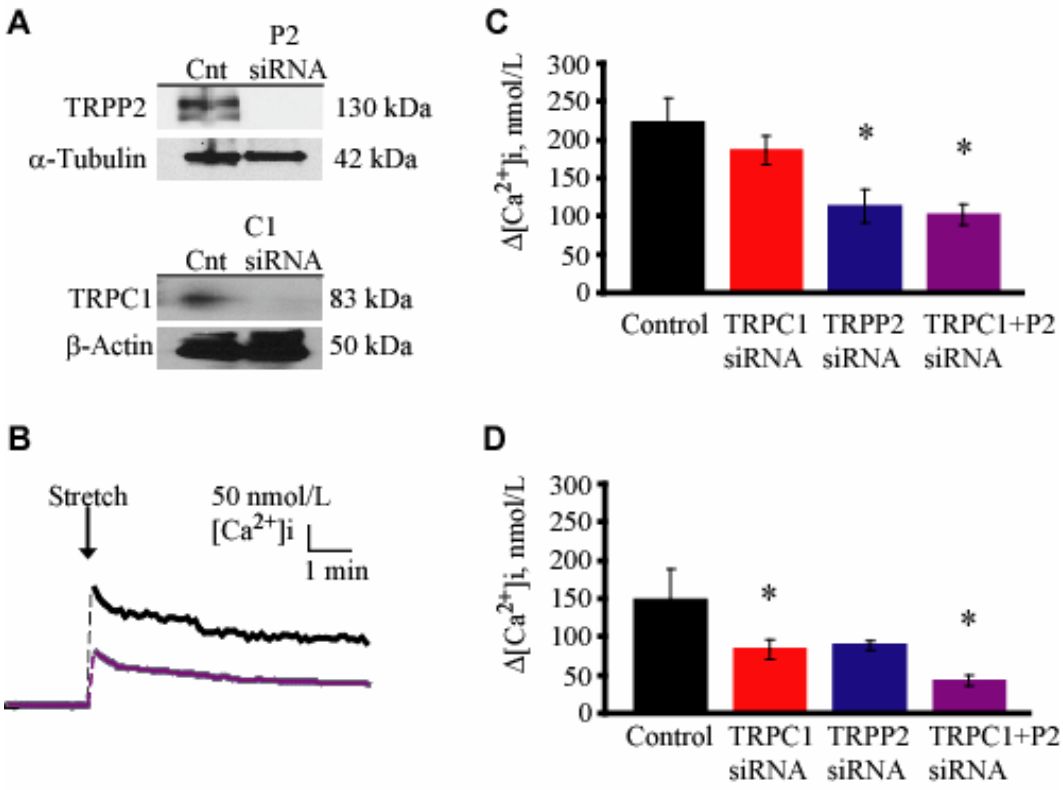


**Figure 3.3. TRPC1 and TRPP2 mediate stretch-induced $[Ca^{2+}]i$ response.**
**A.** Western blot of TRPP2 and TRPC1 protein expression in control (Cnt), TRPP2-targeted siRNA treated (P2 siRNA), and TRPC1-targeted siRNA treated (C1 siRNA) cells. Loading controls ($\alpha$-tubulin and $\beta$-actin) were run in the same lanes on the same gels. **B.** 35% stretch-induced $[Ca^{2+}]i$ response in cells transfected with scrambled siRNA (black trace), or transfected with TRPC1 and TRPP2 targeted siRNA (purple trace). Dashed line in traces represents gap in imaging acquisition. **C.** Summary graph showing the stretch-induced peak response (1 min post-stretch). **D.** Summary graph showing the stretch-induced late response (7 min post-stretch). * $P < 0.05$ vs scramble siRNA control, ANOVA Tukey test). Taken with permission from publisher from (4).

# Chapter Four: TRP channels regulate cytoskeletal and junctional proteins after mechanical stretch

## Background

Restriction of paracellular permeability across the BBB is reliant on the expression and localization of specialized cell junctions, tight junctions, which promote a close relationship between adjacent endothelial membranes (Figure 1.2). Tight junction proteins occludin, claudin (1, 3, 5, and 12), and junctional adhesion molecule (JAM-A, B, and C) are found on brain microvessel endothelial cells (1, 24-25). Following a TBI event, many clinical complications develop including disruption of BBB permeability. Interestingly, experiments on brain microvessel endothelial cells have indicated a correlation between changes in paracellular permeability and alterations in expression of actin filaments (33). Although the mechanism by which the actin cytoskeleton modulates the cell junctions is currently unknown, it has been suggested that actin fibers may provide a necessary tension to enforce a close interlocking of junctions between apposing endothelial membranes (50-52). Actin-myosin contraction, leading to subsequent formation of actin stress fibers, has been reported as a component of endothelial barrier regulation (54-55). Phosphorylation of MLC serves as a trigger to initiate actin-myosin contraction, and is regulated by the activity of MLC kinase and MLC phosphatase (56). Indeed, our lab has previously reported that MLC phosphorylation increases during hypoxia-induced endothelial barrier disruption (57). Several factors have been identified to exert control over MLC phosphorylation, including regulation of MLC phosphatase (through Rho A induced inhibition) and MLC kinase (through intracellular calcium/nitric oxide

dependent activation) (Figure 1.3). In fact, studies have shown that increased levels of [$Ca^{2+}$]i or NO can promote an increase of MLC kinase activity, which subsequently leads to actomyosin contraction(62-65). Intracellular calcium may regulate MLC phosphorylation in a NO-dependent (by activating eNOS to promoting NO synthesis) and NO-independent (by $Ca^{2+}$-calmodulin direct activation of MLC kinase) mechanism. As such, [$Ca^{2+}$]i has been hinted to play an important role in the mechanism underlying loss of BBB integrity following induction of a hypoxic or hypertension injury (57, 66-68). Thus, given the evidence above, in this chapter the activation of downstream signaling mechanisms (related to endothelial barrier disruption) initiated after stretch application was explored.

## Methods

See Chapter 2 methods section for methodology regarding Cell Culture & Solutions, Mechanical Cell Injury, and Statistical Analysis.

### NO measurements

Nitric oxide concentration was measured using fluorescent indicator DAF-FM/AM. Confluent cell cultures were incubated with 5μM DAF-FM/AM (Invitrogen) at room temperature for 1 hour in dark conditions. Following incubation, cells were washed with MBSS solution. Cells were imaged using a Nikon Eclipse TS 100 inverted microscope using a 20X super fluor objective (NA = 0.75) and a 12-bit CCD camera (Pixel Fly, Cooke). Cells loaded with DAF-FM were excited with a 470 nm illumination and the emission monitored at 510 nm. InCyt Im Imaging software was employed for data acquisition and analysis. In each experiment, 10-30 cells were simultaneously monitored and their fluorescence emission averaged at the end of recording.

### Immunocytochemistry

Immuno-staining directed at ppMLC (phosphorylated at Thr18 and Ser19) was used to determine changes in myosin light chain phosphorylated. Cells were grown to confluence on glass cover slips or flexible silastic membranes. Cells were then exposed to desired experimental treatment and subsequently fixed with 4% paraformaldehyde at room temperature. The plasma membrane was

labeled by incubating the cells with tetramethylrhodamine-wheat germ agglutinin (1:200) for 15-20 min at 4˚C prior to permeabilization. Cells were subsequently permeabilized with 0.1% Triton X-100 treatment for 10 min at room temperature. The permeabilized cells were blocked with 1% donkey serum for 30 min at room temperature then incubated with anti-pMLC (1:200, Cell Signaling), for 1.5 hr at room temperature. Cells were then washed and incubated with Cy5 labeled anti-rabbit secondary antibody (1:500-1000) for 30-60 min at room temperature. Cells were mounted on slides using ProLong Gold anti-fade reagent with DAPI nuclear counterstain (Invitrogen). Fixed cells were imaged using the Nikon TiE A1Rsi confocal microscope, and analyzed with NIS Elements imaging software. Measurements of phosphorylated MLC were performed using ImageJ software. Imaging fields were selected based on high cell confluency, and mean fluorescence intensity was measured diagonally across the imaging field (typically across 6-12 cells). For all treatment groups, multiple imaging fields (3-4) were captured from a single fixed membrane. All microscope settings, illumination times, and detection times were held constant for all images and treatment groups.

Similarly, immuno-staining directed at F-actin was used to determine changes in actin stress fiber formation. Confluent cells cultures were exposed to a desired experimental treatment and subsequently fixed with 4% paraformaldehyde at room temperature. The plasma membrane was labeled by incubating cells with tetramethylrhodamine-wheat germ agglutinin (1:200) for 15-20 min at 4˚C, prior to permeabilization. Cells were subsequently permeabilized

with 0.1% Triton X-100 treatment for 10 min at room temperature. Subsequently, cells were blocked with 1% donkey serum for 30 min at room temperature, then incubated with anti-TRPP2 (1:100, Santa Cruz Biotechnology), or anti-TRPC1 (1:100, Santa Cruz Biotechnology) at room temperature for 1 hr. Cells were then washed and incubated with Cy2 labeled anti-rabbit secondary antibody (1:400) or Alexa Fluor 647 phalloidin (1:1000, Invitrogen) for 30-60 min at room temperature. Cells were then treated with ProLong Gold anti-fade reagent with DAPI nuclear counterstain (Invitrogen), and mounted on glass slides. Fixed cells were imaged using the Nikon TiE A1Rsi confocal microscope, and analyzed with NIS Elements imaging software. Measurements of actin stress fiber formation were performed using ImageJ software. Imaging fields were selected based on high cell confluency, and the mean fluorescence intensity was measured diagonally across the imaging field (typically across 6-12 cells). For all treatment groups, multiple imaging fields (2-3) were captured from a single fixed membrane and the mean intensity was averaged for an n of 1. All microscope settings, illumination times, and detection times were held constant for all images and treatment groups.

## Results

### TRP channels mediate stretch-induced NO synthesis

Recently several studies have identified nitric oxide signaling as an important modulator of endothelial barrier integrity through regulation of the actin cytoskeleton (56, 62-64). As intracellular calcium is known to increase nitric oxide synthesis through activation of endothelial nitric oxide synthase, we investigated whether nitric oxide levels were influenced by the observed stretch-induced $[Ca^{2+}]i$ dynamic. Indeed, we found that stretch application resulted in a rapid increase in DAF-FM fluorescence, a molecule that increases its fluorescent intensity when it reacts with NO, leading to an increase in $F/F_o$ of 52 ± 11, n = 9 (Figure 4.1A, E). In addition, when cells were pre-treated (30 minutes, 100 μM) with nitric oxide synthase inhibitor, L-NAME, the application of stretch failed to yield an increase in DAF-FM fluorescence (Figure 4.1B, E). Thus, it seems apparent that stretch application results in a state of elevated NO synthesis by activation of nitric oxide synthase.

We further examined whether nitric oxide synthase activation was dependent on TRP channel mediated calcium influx. Treatment with TRPC inhibitor, LOE908 (10 μM), promptly led to a reduction of the stretch-induced NO synthesis (-15 ± 12 % $F/F_o$ of control, n = 4, Figure 4.1C, E). Likewise, application of amiloride, a non-specific TRPP2 inhibitor, also decreased the stretch-induced NO increase (-0.5 ± 12 % $F/F_o$ of control, n = 5, Figure 4.1D-E).

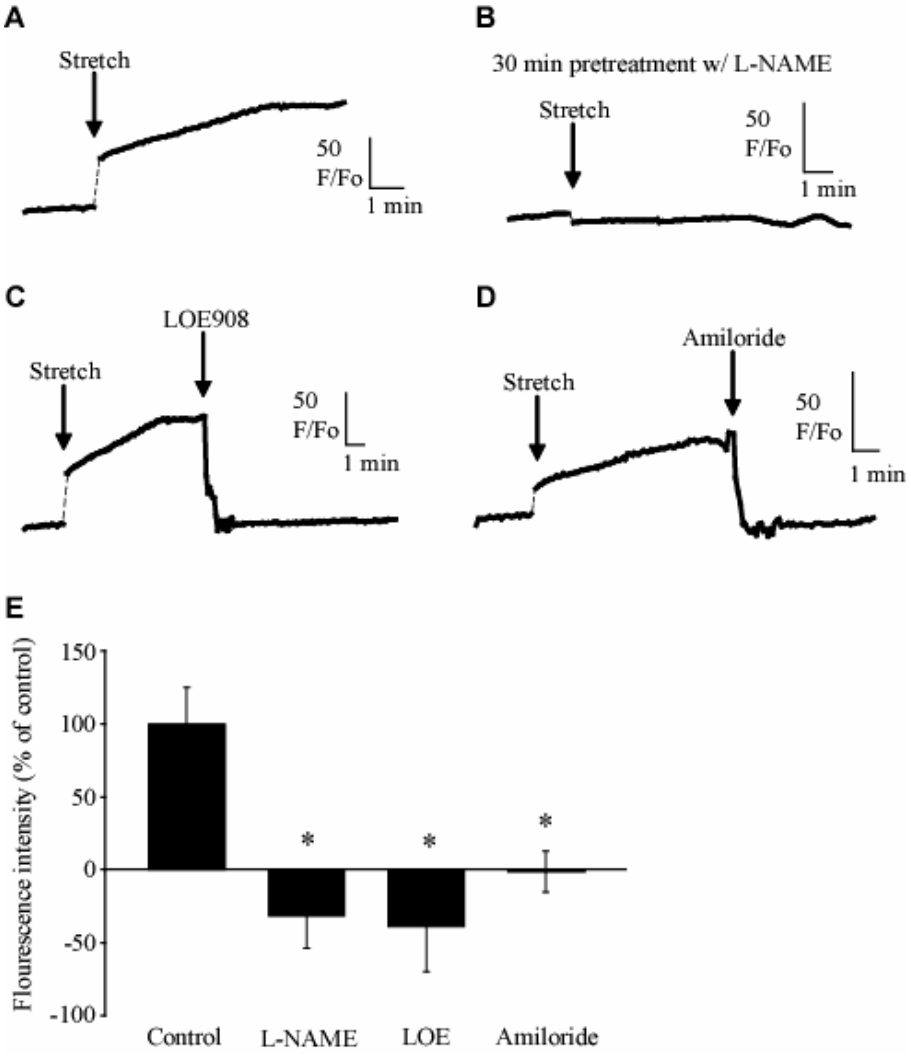


**Figure 4.1. Stretch induced NO synthesis.**
Traces are representative of fluorescent intensity recordings from cells loaded with DAF-FM ($F/F_o$). **A.** Application of 35% stretch generated an increase of NO. **B.** Application of stretch following 30 minute pre-treatment with 100 μmol/L L-NAME (NOS inhibitor). **C.** Stretch followed by application of 10μmol/L LOE908. **D.** Stretch followed by application of 10μmol/L amiloride. **E.** Summary bar graph showing mean changes in DAF-FM fluorescent intensity after stretch application in control (n = 9), after treatment with L-NAME (n = 4), LOE908 (n = 4), and amiloride (n = 5).(* $P < 0.05$ vs no treatment control, ANOVA Tukey test) Dashed line in traces represents gap in imaging acquisition. Taken with permission from publisher from (4).

Hence, the mechanosensitive TRP channels, TRPC1 and TRPP2, activated by stretch appear to mediate NO synthesis through activation of eNOS.

**NO effect on the stretch-induced $[Ca^{2+}]i$ response**

NO has been reported to modulate the activity of various proteins including some ion channels (58-59, 122-123). In fact, experiments have demonstrated that TRPC5 is activated by NO through modification of cysteine residues (Cys 553, Cys 558) residing within the pore-forming region (between the $5^{th}$ and $6^{th}$ transmembrane domain) (124-125). Further, several other TRP channels, including TRPC1, also contain similarly located cysteine residues. Therefore, we next explored the possibility that the stretch-induced NO increase might exert some control over the $[Ca^{2+}]i$ response. We observed that application of NO donor, SNAP (100 μM), failed to produce a significant increase of $[Ca^{2+}]i$, displaying a peak increase of 12 ± 3 nM (n = 4) (Figure 4.2A, C). This demonstrates that NO does not, by its self, mediate activation of calcium permeable channels in our brain endothelial cell cultures. In agreement, 30 minute pre-incubation with NOS inhibitor, L-NAME (100 μM), did not lead to any reduction of the stretch-induced $[Ca^{2+}]i$ dynamic, but rather it led to a significant increase of the peak $[Ca^{2+}]i$ response (297 ± 31 nM, n = 3) compared to control (Figure 4.2B-C). Thus, the stretch-induced NO increase does not seem to mediate the activation of TRPC1 and TRPP2, as has been reported for other TRP channels. The increase $[Ca^{2+}]i$ response suggests that NO is responsible for mediating mechanisms to reduce cytosolic calcium following stretch.

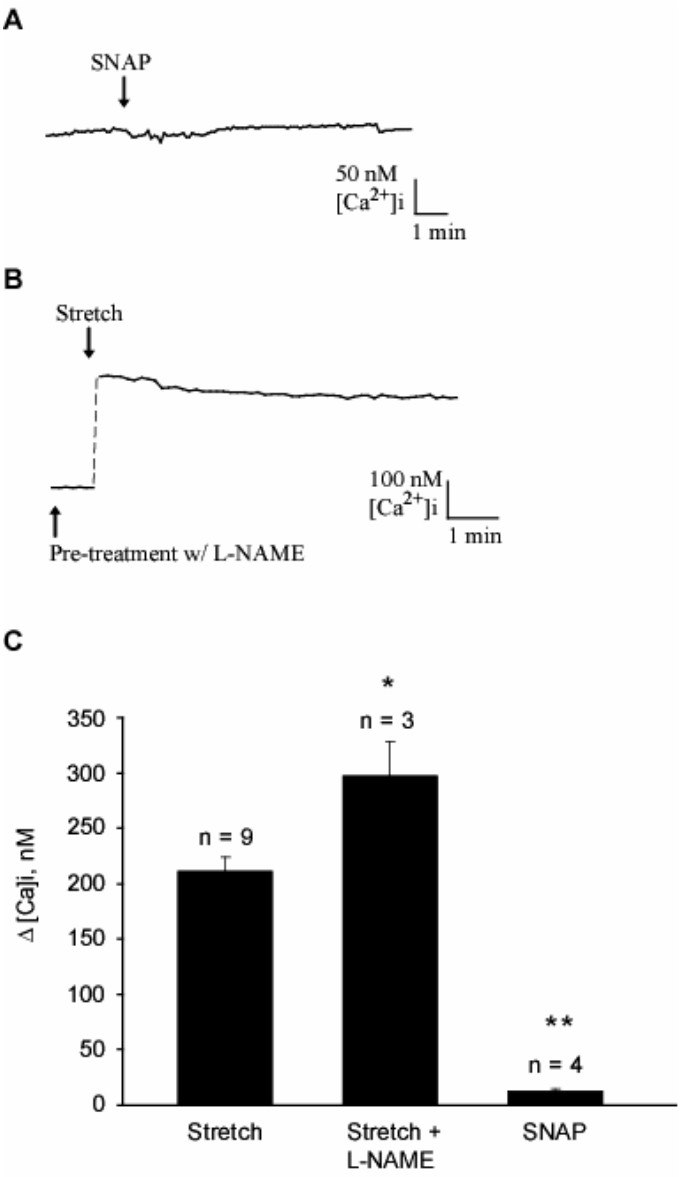


**Figure 4.2. NO mediated $[Ca^{2+}]i$ dynamics.**
**A.** Application of NO donor, 100 mM SNAP generated a minimal change of the $[Ca^{2+}]i$. **B.** Application of 35% stretch under control following 30 minutes of pre-treatment with 100 μM L-NAME. Dashed line in trace represents gap in imaging acquisition. **C.** Summary bar graph showing the peak increase of $[Ca^{2+}]i$ after 35% stretch plus or minus L-NAME pretreatment and SNAP application.

**Stretch-induced MLC phosphorylation**

Interestingly $[Ca^{2+}]i$ and NO have both been reported to increase myosin light chain kinase activity and thus promote actomyosin contractility. We therefore investigated whether there was a change in the phosphorylated myosin level after stretch. We found that exposure of brain endothelial cells to stretch led to a significant increase in phosphorylated myosin 10 minutes post-stretch (Figure 4.3A-B). In addition, pretreatment with 10μM LOE908 and 10μM amiloride was effective in preventing the stretch-induced MLC phosphorylation, suggesting that the TRP channel mediated $[Ca^{2+}]i$ influx is critical for stretch-induced actomyosin contractility (Figure 4.3A-B). Further, pre-incubation with L-NAME (100 μM, 30 minutes) also resulted in a repression of the stretch-induced MLC phosphorylation (Figure 4.3A, C). Thus, it seems that TRP channel mediated NO generation is necessary for modulation of the cytoskeleton after stretch application.

**Stretch-induced stress fiber formation**

Actomyosin contractility, through MLC phosphorylation, is linked to loss of integrity of the endothelial barrier (57). Formation of actin stress fibers is reported to be a result of phosphorylated-MLC mediated actin cytoskeletal rearrangement (126-128). Hence, we explored whether formation of actin stress fibers was apparent following stretch. Phalloidin, Alexa Fluor 647, was used to label actin stress fibers prior to stretch application as well as 2, 10, 15, 30, and 60 min post-stretch. Application of stretch demonstrated a trend for stress fiber formation up

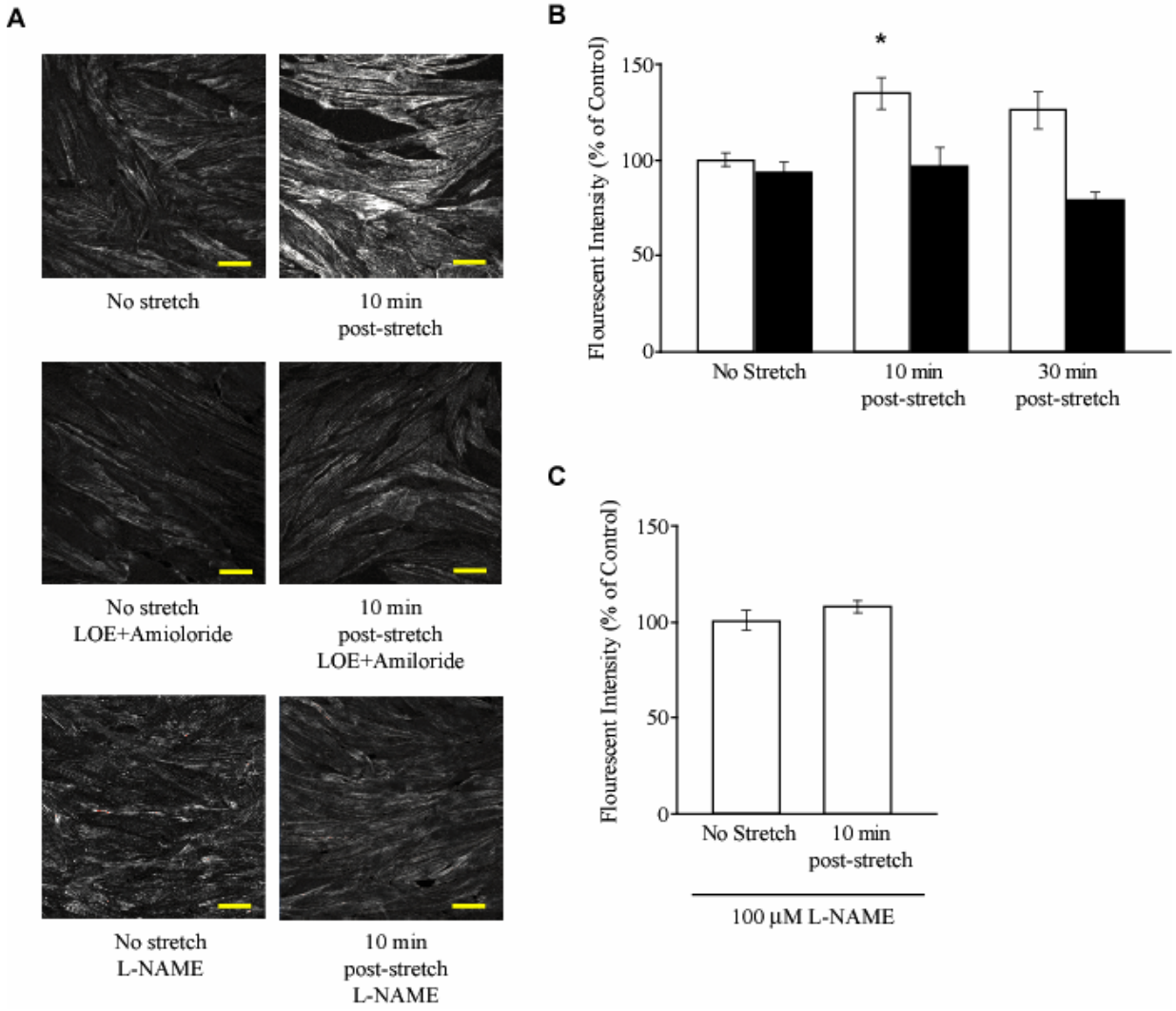


**Figure 4.3. TRP mediated MLC phosphorylation.**
**A.** Representative pictures of phosphorylated MLC (in white) under various treatment conditions. Scale bar (yellow) is representative of 10 μm. **B.** Summary bar graph of pMLC fluorescence intensity measurements in cells exposed to control mechanical stretch (white bars) or 10 minutes of pretreatment with 10μM LOE908 and 10μM amiloride followed by mechanical stretch (black bar). **C.** Summary bar graph of pMLC fluorescence intensity measurements in cells exposed to mechanical stretch after 30 minutes of pretreated with 100μM L-NAME.

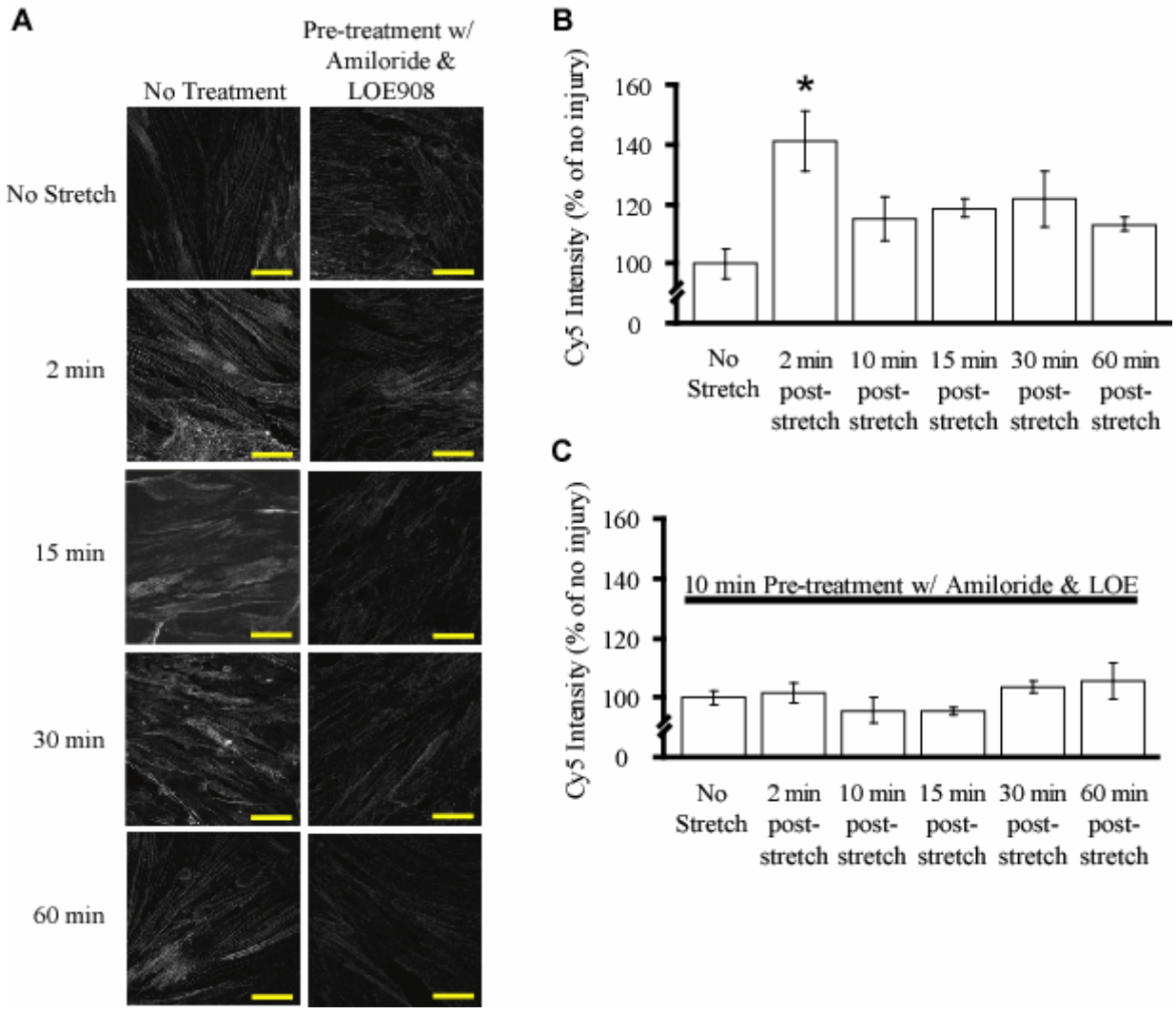


**Figure 4.4. TRP mediated actin stress fiber formation.**
**A.** Representative pictures of actin stress fibers (in white) under various treatment conditions. Scale bar (yellow) is representative of 10 μm. **B-C.** Summary graphs showing effect of stretch on f-actin staining fluorescent intensity in (**B**) untreated cells and (**C**) cells treated with 10 μM amiloride and 10 μM LOE908 10 minutes prior to stretch application. Taken with permission from publisher from (4).

to an hour post-stretch, with the largest apparent phalloidin fluorescence at 2 min post-stretch (41 ± 10 percent increase from control, n = 3) (Figure 4.4A-B). Further, 10 minute pre-treatment with TRP channel inhibitors, LOE908 (10 μM) and amiloride (10 μM), abolished any tendency for stretch-induced actin stress fiber formation (Figure 4.4A, C). Thus, it appears that the stretch-induced $[Ca^{2+}]i$ increase, mediated by TRPC1 and TRPP2, leads to generation of stress fibers and rearrangement of the actin cytoskeleton.

**Stretch-induced tight junction modification**

Changes in endothelial barrier permeability are believed to be primarily regulated by the integrity of the tight junction complexes. Previous works have demonstrated the importance of claudin 5 expression to the proper maintenance of BBB integrity (35). In fact, experiments using claudin 5 knockouts showed the establishment of a BBB with a size selective increase in paracellular permeability (36), suggesting that claudin 5 does not appear to be a critical protein for the establishment of the BBB. It may however serve as an important fine tune control to regulate permeability. Thus, we investigated the effect of that mechanical stretch may have on claudin 5 in our brain microvessel endothelial cells. We found that application of stretch did not yield any significant change in claudin 5 localization at the plasma membrane up to 60 minutes post stretch (Figure 4.5A). Hence, it does not appear as though mechanical stretch application has an effect on claudin 5 expression.

ZO-1 serves as a critical component of the tight junction complex, linking tight junction proteins to the actin cytoskeleton. Recently, several studies have reported changes in ZO-1 expression following alteration of the actin cytoskeleton (39, 41). Further, decreased ZO-1 expression at the plasma membrane (near tight junctions) has been shown to promote a decrease of barrier integrity (40). Therefore, we explored whether mechanical stretch induced a decrease in plasma membrane ZO-1 expression. We found that application of stretch did not induce a significant decrease in ZO-1 localization at the plasma membrane (Figure 4.5B). Rather, we observed an increase of ZO-1 membrane localization at 30 minutes post stretch. It is possible that the increase observed may serve as a compensatory response to reestablish a disrupted junctional component which we were not able to detect.

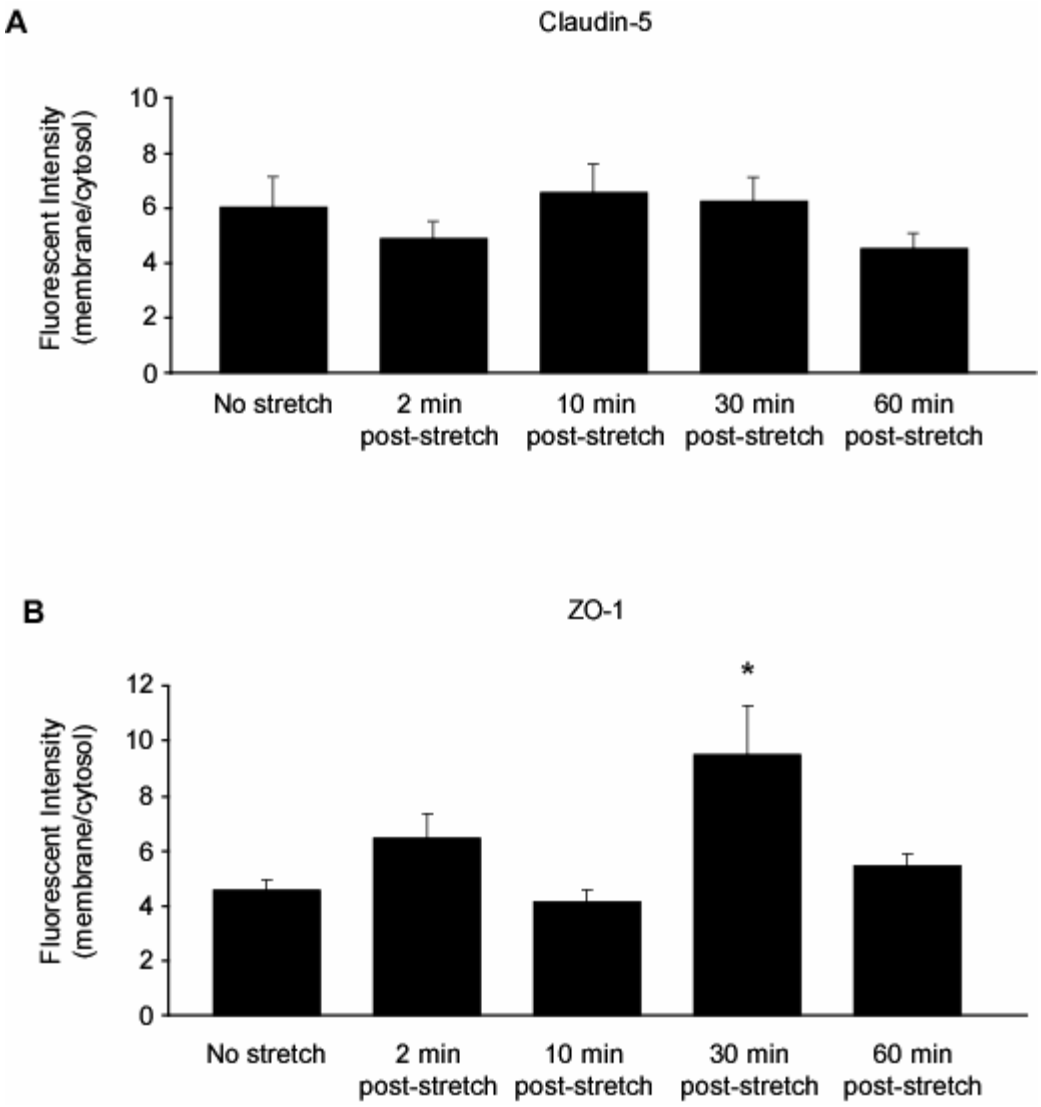


**Figure 4.5. Effect of stretch on TJ localization.**
**A.** Summary bar graph of Claudin 5 fluorescence intensity measurements in cells exposed to mechanical stretch. **B.** Summary bar graph of ZO-1 fluorescence intensity measurements in cells exposed to mechanical stretch.

# Chapter Five: Discussion

**Mechanical stretch triggers an increase of intracellular calcium in brain endothelial cells**

TBI leads to the development of various detrimental conditions including disruption of the cerebral microvasculature. Under this state the BBB loses its integrity and allows for greater paracellular permeability, which can result in deleterious alteration of the CNS interstitial fluid. Despite a great lack of understanding as to the mechanism responsible for the TBI-induced dysregulation of the endothelial cell barrier, evidence exists implicating $[Ca^{2+}]i$ as a major factor underlying modulation of the BBB integrity. Indeed, several studies have shown that inhibition of calcium permeable channels results in protection of the BBB integrity against hypoxic or hypertension insult (57, 66-68). Therefore, an aim of this work was to characterize the $[Ca^{2+}]i$ dynamics that arise in brain microvessel endothelial cells following exposure to mechanical stress (in the range believed to be relevant to TBI).

As TBI is believed to result in linear tension (stretch) on the cells, we employed a model of mechanical stretch, Cell Injury Controller II, for the purpose of applying TBI-mimicking mechanical stress on cells. In this model, cells were exposed to rapid, 50 ms, bi-axial stretch with the degree of strain being set by the extent of elongation of the elastic membrane (see Figure 2.1). Previous work has demonstrated that elastic membrane elongation of 35-55% results in cell damage and apoptosis in astrocyte cell cultures (114). Similarly, application of 35-55% stretch induced apoptosis in neuronal cell cultures; with the proportion of cell

damage increasing as the degree of stretch was incremented (129-130). It is worth noting however, that endothelial cells may not be as susceptible to stretch-induced cell damage since exposure of aortic endothelial cells to stretch (in the range of 54-180% stretch) yielded a greatly diminished amount of apoptosis, as compared to the levels seen for astrocytes and neurons (130). Hence, we expect that in our experiments the application of 35-55% stretch likely resulted in minor damage to the population of endothelial cells.

Our data revealed that application of mechanical stretch induced an $[Ca^{2+}]i$ increase. A typical stretch-induced calcium dynamic consisted of two components, an initial transient increase followed by a prolonged $[Ca^{2+}]i$ increase. In addition, the amplitude of the $[Ca^{2+}]i$ response is dependent on the degree of stretch applied. Stretch application of 10% or lower failed to evoke an $[Ca^{2+}]i$ increase, and progressively elevated stretch levels yielded increasing $[Ca^{2+}]i$ responses. This is in agreement with reports of mechanical stretch application to neurons and astrocytes, in which case a similar prolonged $[Ca^{2+}]i$ dynamic was reported and the observed $[Ca^{2+}]i$ increase was sensitive to the degree of stretch applied (114-115, 131). Furthermore, experimental manipulation of the extracellular calcium pool and intracellular calcium stores revealed that extracellular calcium influx largely is responsible for the stretch-induced $[Ca^{2+}]i$ dynamic. Whereas calcium release from intracellular stores seems to only contribute marginally to the initial transient increase, extracellular calcium influx appears to mediate both a great portion of the initial transient as well as the sustained $[Ca^{2+}]i$ increase.

Although It is still unclear which calcium-permeable channels are responsible for the observed calcium release from intracellular stores, a few likely suspects exist. The inositol triphosphate receptor (IP3R) is one such candidate, as it has been reported to be express in brain microvessel endothelial cells and phospholipase C activity (which generates the IP3R ligand, IP3) is reported to increase in response to mechanical stress and $[Ca^{2+}]i$ elevation (132-134). In addition, the ryanodine receptors (RyR) are another candidate since they have also been shown to be expressed in brain microvessel endothelial cells and are activated by intracellular calcium (135). Further, TRP channels could also play a role in calcium release from intracellular stores since several are known to express on the endoplasmic reticulum membrane. Since several strong candidates exist future work will be required to uncover the identity of the channel(s) which mediate the stretch-induced store release.

**TRP channels mediate calcium signaling after mechanical stretch**

Investigation to ascertain the identity of the calcium-permeable channel(s) mediating influx of extracellular calcium following stretch application revealed that TRP channels, TRPC1 and TRPP2, mediated a large portion of the stretch-induced $[Ca^{2+}]i$ response. Indeed, simultaneous knockdown, of TRPC1 and TRPP2 protein expression, led to a significant, major reduction of the stretch-induced $[Ca^{2+}]i$ dynamic throughout our recording (over the course of several minutes). Hence, our data suggest that these mechanosensitive channels display

prolonged activation following stretch, allowing for continuous extracellular calcium influx. A potential explanation for this prolonged TRP channel activation is that TRPC1 and TRPP2 may have a functional coupling to calcium-activated potassium ($K_{Ca}$) channels which may also be activated post-stretch. Evidence exists to showing that $K_{Ca}$ channels associate with TRP channels, and that $K_{Ca}$ channel activation may mediate TRP channel opening (136-138). Indeed, a study on prostate cancer cells revealed that the intermediate-conductance $K_{Ca}$ (IK) channel shared a physical coupling to TRPV6 and that activation of the IK channel was sufficient to cause a sustained TRPV6 mediated $[Ca^{2+}]i$ increase (over the course of several minutes) (139). It has been suggested that potassium channel activation may hyperpolarize the cell and result in a state favoring TRP channel mediated $Ca^{2+}$-influx (136, 140). Since brain microvessel endothelial cells are reported to express large, intermediate, and small $K_{Ca}$ channels (MaxiK, IK, and SK2) (141-143), it may be that these potassium channels play a role in the prolonged stretch-induced $[Ca^{2+}]i$ response.

The duration of the stretch-induced $[Ca^{2+}]i$ dynamic and its overall significance to the progression of TBI remain largely unclear. Our data suggest that the stretch-induced $[Ca^{2+}]i$ dynamic likely persists for hours, since the $[Ca^{2+}]i$ response appeared to be sustained up to one hour post-stretch. In agreement, studies investigating the effect of mechanical stress on neurons and astrocytes demonstrated that $[Ca^{2+}]i$ remains high for several hours (114, 131). Indeed, Weber et al showed that in neurons application of 35% stretch induced a $[Ca^{2+}]i$

response that progressed for three hours, and 55% stretch induced a $[Ca^{2+}]i$ response with a duration of five hours (115).

An interesting aspect of the stretch-induced response is the mechanical activation of TRPC1 and TRPP2. Recent studies indicate that TRPC1 may be activated in a bi-layer dependent manner (see Chapter 1 – Mechanical sensation), where tension applied to the lipid membrane leads to channel activation (89, 94, 96). Thus it stands that following stretch application, in our experiments, TRPC1 may be activated in a similar fashion. However, the mechanical activation of TRPP2 appears less clear. TRPP2 is reported to have no mechanosensitive properties when expressed alone (104). The documented activation by mechanical stress of TRPP2 is attributed to its association with mechanosensitive proteins. Indeed, in the kidney TRPP2 has been shown to couple with polycystin kidney disease 1 (PKD1), a mechanosensitive protein, to mediate $[Ca^{2+}]i$ dynamics in response to shear stress (102-104). In addition, TRPP2 has also been reported to form a mechanosensitive channel when expressed as a heterotetramer with TRPV4 (102, 144). Yet, PKD1 does not appear to be expressed in our brain microvessel endothelial cells (no mRNA was detected, see Figure 3.1), and the TRPV channel antagonist (ruthenium red, see Figure 3.2) failed to show a significant reduction of the $[Ca^{2+}]i$ response. Hence, it seems probable that TRPP2 mechanical activation is due to its coupling to another mechanosensitive protein. Interestingly, TRPC1 has recently been reported to form a channel with TRPP2 (145-148). Although the mechanosensitive properties of the TRPC1-TRPP2 heterotetramer have not

been identified, it may be the case that in brain microvessel endothelial cells the stretch-induced activation of TRPP2 is mediated through its association with a mechanosensitive protein (potentially TRPC1).

**TRP channels regulate cytoskeletal and junctional proteins after mechanical stretch**

We further examined whether the stretch-induced $[Ca^{2+}]i$ dynamic initiated downstream signaling which may result in regulation of the endothelial barrier. We found that the stretch-induced TRP channel activation resulted in an increase in the production of NO. In addition, we found that MLC phosphorylation and actin stress fiber formation increased after stretch, and both events were dependent on TRC channel activation and NO synthesis. Recently, several studies have suggested that the actin cytoskeleton plays an important role in regulating the integrity of endothelial tight junctions, and hence barrier permeability (48-49). As such, studies of brain microvessel endothelial cells have indicated a correlation between changes in paracellular permeability and alterations in expression of actin filaments (33). In addition actin-myosin contraction, leading to subsequent formation of actin stress fibers, has been reported as a component of endothelial barrier regulation (55, 128).

Phosphorylation of MLC serves as a trigger to initiate actin-myosin contraction, and is regulated by the activity of MLC kinase and MLC phosphatase (56). Our lab has previously demonstrated that, under hypoxic conditions, TRPC channels may regulate BBB integrity through actomyosin cytoskeletal

modification brought on by MLC phosphorylation (57). Several factors have been identified to exert control over MLC phosphorylation, including intracellular calcium and NO dependent activation regulation of MLC kinase. Indeed, accumulating evidence points to an NO-mediated modulation of barrier permeability in endothelial cells through mechanisms involving actin-cytoskeleton modifications (56, 62-64). In addition, multiple studies have shown that increased levels of $[Ca^{2+}]i$ may promote increase of MLC kinase activity, subsequently leading to actomyosin contraction (56, 65). Therefore, we reason that mechanical activation of endothelial TRP channels, TRPC1 and TRPP2, leads to a rise in $[Ca^{2+}]i$ and subsequently signals an increase of NO synthesis through activation of eNOS. NO then may stimulate myosin light chain kinase activity. And as a consequence promote increased phosphorylation of MLC resulting in contraction of the actin-myosin cytoskeleton, formation of actin stress fibers, and diminished barrier integrity (149-150) (Figure 5.1).

Although the mechanism by which the actin cytoskeleton modulates the cell junctions is currently unknown, it has been suggested that actin fibers may provide a necessary tension to enforce a close interlocking of junctions between apposing endothelial membranes. We investigated whether stretch application led to relocalization of tight junction complex proteins, claudin 5 and ZO-1. In our experiments, immunofluorescence imaging studies did not show evidence of a significant change in claudin 5 localization, up to an hour following stretch application. Similarly, no reduction of ZO-1 localization at the cell membrane was apparent, although we did observe an increase at 30 minutes post-stretch. The

increase observed, at 30 minutes post-stretch, may be representative of a compensatory response to reestablish a disrupted junctional component which we were not able to detect. Despite not detecting a significant loss of tight junction protein expression at the membrane, the identification of alteration to the actin cytoskeleton (increase phosphorylated MLC and stress fiber formation) suggests that the mechanical stretch-induced response likely results in modification of the endothelial barrier permeability. It seems likely that changes in endothelial barrier permeability have occurred following stretch application, however these changes may not lead to a marked alteration in localization of tight junction proteins. The use of this stretch model, while advantageous for the induction of TBI-mimicking mechanical stress, impeded the direct assessment of barrier permeability. As such, future studies will aim to more directly assess the interplay between endothelial paracellular permeability, tight junction expression/localization, and mechanical stretch application.

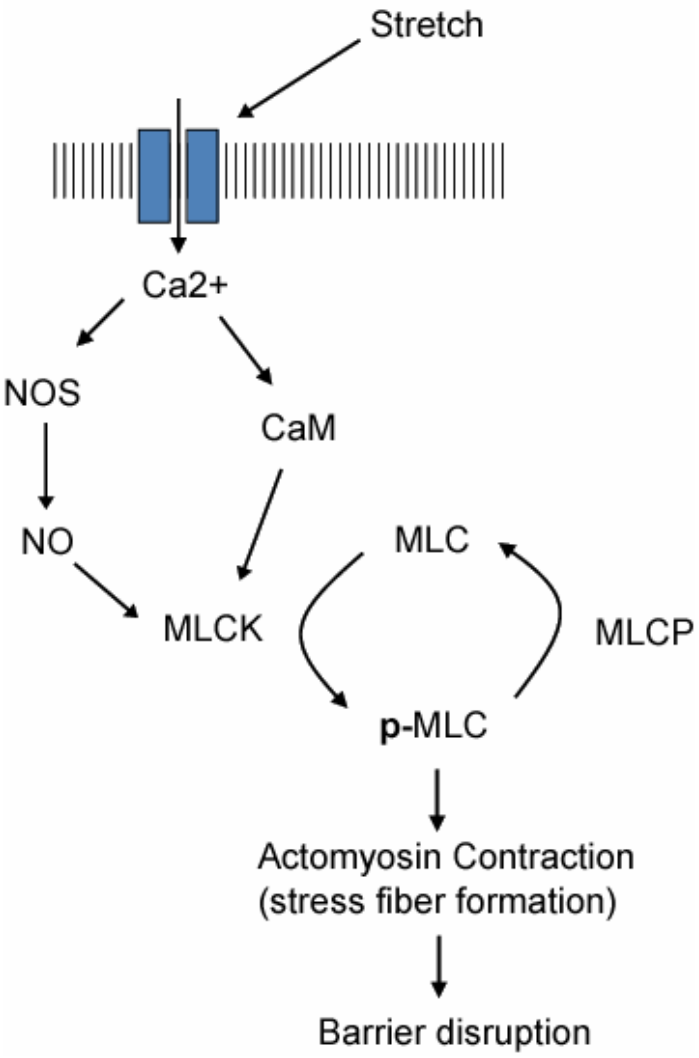


**Figure 5.1 Summary of stretch-induced signaling.**
Diagram depicting the signaling response initiated in bEnd3 cells following application of mechanical stretch.

# Conclusion & Significance

In conclusion, this research project has served to characterize the calcium-signaling response of brain endothelial cell to mechanical stress levels that are thought to reflect those experienced during TBI. We report that in our experiments, application of stretch injury caused endothelial cells to undergo a modest calcium release from intracellular stores in addition to a prolonged influx of extracellular calcium. Further, we identified two calcium-permeable ion channels, TRPP2 and TRPC1, which are largely responsible for the prolonged stretch-induced $[Ca^{2+}]i$ dynamics. We found that this intracellular calcium increase led to activation of eNOS and consequently led to an increase of NO synthesis. We further identified a rise of phosphorylated MLC levels after stretch, which appears to be dependent on TRP channel activation and NO synthesis. Furthermore, we observed an increase of actin stress fiber formation following stretch application, which was dependent on TRP channel mediated calcium influx. Suggesting that stretch application may induce an alteration of the actin cytoskeleton. Thus it appears that TRP channels, TRPC1 and TRPP2, may serve as important mediators of the TBI induced alteration of brain microvessel endothelial cell permeability. Future work will attempt to better characterize the mechanism of TRP channel mechanosensation and the change in barrier permeability induced by mechanical stretch. Much work still needs to be done before a complete picture of “how the microvasculature is affected by TBI” is available, however the findings uncovered in this research project has added new pieces to that puzzle.

**Bibliography**

1. Huber, J. D., R. D. Egleton, and T. P. Davis. 2001. Molecular physiology and pathophysiology of tight junctions in the blood-brain barrier. Trends Neurosci 24:719-725.

2. McCarty, J. H. 2005. Cell biology of the neurovascular unit: implications for drug delivery across the blood-brain barrier. Assay Drug Dev Technol 3:89-95.

3. Persidsky, Y., S. H. Ramirez, J. Haorah, and G. D. Kanmogne. 2006. Blood-brain barrier: structural components and function under physiologic and pathologic conditions. J Neuroimmune Pharmacol 1:223-236.

4. Berrout, J., M. Jin, and R. G. O'Neil. 2012. Critical role of TRPP2 and TRPC1 channels in stretch-induced injury of blood-brain barrier endothelial cells. Brain Res 1436:1-12.

5. Perlmutter, L. S., and H. C. Chui. 1990. Microangiopathy, the vascular basement membrane and Alzheimer's disease: a review. Brain Res Bull 24:677-686.

6. Abbott, N. J., L. Ronnback, and E. Hansson. 2006. Astrocyte-endothelial interactions at the blood-brain barrier. Nat Rev Neurosci 7:41-53.

7. Armulik, A., G. Genove, and C. Betsholtz. 2011. Pericytes: developmental, physiological, and pathological perspectives, problems, and promises. Dev Cell 21:193-215.

8. Lai, C. H., and K. H. Kuo. 2005. The critical component to establish in vitro BBB model: Pericyte. Brain Res Brain Res Rev 50:258-265.

9. Capaldo, C. T., and A. Nusrat. 2009. Cytokine regulation of tight junctions. Biochim Biophys Acta 1788:864-871.

10. Herbert, S. P., and D. Y. Stainier. 2011. Molecular control of endothelial cell behaviour during blood vessel morphogenesis. Nat Rev Mol Cell Biol 12:551-564.

11. Abbott, N. J., and P. A. Revest. 1991. Control of brain endothelial permeability. Cerebrovasc Brain Metab Rev 3:39-72.

12. Crone, C., and S. P. Olesen. 1982. Electrical resistance of brain microvascular endothelium. Brain Res 241:49-55.

13. Zlokovic, B. V. 1995. Cerebrovascular permeability to peptides: manipulations of transport systems at the blood-brain barrier. Pharm Res 12:1395-1406.

14. Goldmann, E. 1913. Vitalfarburg am zentralnervensystem. Abhandl Konigl preuss Akad Wiss 1:1-60.

15. Bradbury, M. W. B. 1979. The Concept of a Blood-Brain Barrier. Chichester.

16. Cserr, H. F., and M. Bundgaard. 1984. Blood-brain interfaces in vertebrates: a comparative approach. Am J Physiol 246:R277-288.

17. Weiss, N., F. Miller, S. Cazaubon, and P. O. Couraud. 2009. The blood-brain barrier in brain homeostasis and neurological diseases. Biochim Biophys Acta 1788:842-857.

18. Engelhardt, B., and L. Sorokin. 2009. The blood-brain and the blood-cerebrospinal fluid barriers: function and dysfunction. Semin Immunopathol 31:497-511.

19. Hosoya, K., and M. Tachikawa. 2011. Roles of organic anion/cation transporters at the blood-brain and blood-cerebrospinal fluid barriers involving uremic toxins. Clin Exp Nephrol 15:478-485.

20. Patel, M. M., B. R. Goyal, S. V. Bhadada, J. S. Bhatt, and A. F. Amin. 2009. Getting into the brain: approaches to enhance brain drug delivery. CNS Drugs 23:35-58.

21. Girardin, F. 2006. Membrane transporter proteins: a challenge for CNS drug development. Dialogues Clin Neurosci 8:311-321.

22. Miller, D. S. 2010. Regulation of P-glycoprotein and other ABC drug transporters at the blood-brain barrier. Trends Pharmacol Sci 31:246-254.

23. Urquhart, B. L., and R. B. Kim. 2009. Blood-brain barrier transporters and response to CNS-active drugs. Eur J Clin Pharmacol 65:1063-1070.

24. Brightman, M. W., and T. S. Reese. 1969. Junctions between intimately apposed cell membranes in the vertebrate brain. J Cell Biol 40:648-677.

25. Nagasawa, K., H. Chiba, H. Fujita, T. Kojima, T. Saito, T. Endo, and N. Sawada. 2006. Possible involvement of gap junctions in the barrier function of tight junctions of brain and lung endothelial cells. J Cell Physiol 208:123-132.

26. Feldman, G. J., J. M. Mullin, and M. P. Ryan. 2005. Occludin: structure, function and regulation. Adv Drug Deliv Rev 57:883-917.

27. Saitou, M., Y. Ando-Akatsuka, M. Itoh, M. Furuse, J. Inazawa, K. Fujimoto, and S. Tsukita. 1997. Mammalian occludin in epithelial cells: its expression and subcellular distribution. Eur J Cell Biol 73:222-231.

28. Sakakibara, A., M. Furuse, M. Saitou, Y. Ando-Akatsuka, and S. Tsukita. 1997. Possible involvement of phosphorylation of occludin in tight junction formation. J Cell Biol 137:1393-1401.

29. Wachtel, M., K. Frei, E. Ehler, A. Fontana, K. Winterhalter, and S. M. Gloor. 1999. Occludin proteolysis and increased permeability in endothelial cells through tyrosine phosphatase inhibition. J Cell Sci 112 ( Pt 23):4347-4356.

30. Plumb, J., S. McQuaid, M. Mirakhur, and J. Kirk. 2002. Abnormal endothelial tight junctions in active lesions and normal-appearing white matter in multiple sclerosis. Brain Pathol 12:154-169.

31. Dallasta, L. M., L. A. Pisarov, J. E. Esplen, J. V. Werley, A. V. Moses, J. A. Nelson, and C. L. Achim. 1999. Blood-brain barrier tight junction disruption in human immunodeficiency virus-1 encephalitis. Am J Pathol 155:1915-1927.

32. Davies, D. C. 2002. Blood-brain barrier breakdown in septic encephalopathy and brain tumours. J Anat 200:639-646.

33. Mark, K. S., and T. P. Davis. 2002. Cerebral microvascular changes in permeability and tight junctions induced by hypoxia-reoxygenation. Am J Physiol Heart Circ Physiol 282:H1485-1494.

34. Schneeberger, E. E., and R. D. Lynch. 2004. The tight junction: a multifunctional complex. Am J Physiol Cell Physiol 286:C1213-1228.

35. Andras, I. E., and M. Toborek. 2011. HIV-1-induced alterations of claudin-5 expression at the blood-brain barrier level. Methods Mol Biol 762:355-370.

36. Nitta, T., M. Hata, S. Gotoh, Y. Seo, H. Sasaki, N. Hashimoto, M. Furuse, and S. Tsukita. 2003. Size-selective loosening of the blood-brain barrier in claudin-5-deficient mice. J Cell Biol 161:653-660.

37. Furuse, M. 2010. Molecular basis of the core structure of tight junctions. Cold Spring Harb Perspect Biol 2:a002907.

38. Fanning, A. S., and J. M. Anderson. 2009. Zonula occludens-1 and -2 are cytosolic scaffolds that regulate the assembly of cellular junctions. Ann N Y Acad Sci 1165:113-120.

39. Jiao, H., Z. Wang, Y. Liu, P. Wang, and Y. Xue. 2011. Specific role of tight junction proteins claudin-5, occludin, and ZO-1 of the blood-brain barrier in a focal cerebral ischemic insult. J Mol Neurosci 44:130-139.

40. Umeda, K., J. Ikenouchi, S. Katahira-Tayama, K. Furuse, H. Sasaki, M. Nakayama, T. Matsui, S. Tsukita, and M. Furuse. 2006. ZO-1 and ZO-2 independently determine where claudins are polymerized in tight-junction strand formation. Cell 126:741-754.

41. Van Itallie, C. M., A. S. Fanning, A. Bridges, and J. M. Anderson. 2009. ZO-1 stabilizes the tight junction solute barrier through coupling to the perijunctional cytoskeleton. Mol Biol Cell 20:3930-3940.

42. Umeda, K., T. Matsui, M. Nakayama, K. Furuse, H. Sasaki, M. Furuse, and S. Tsukita. 2004. Establishment and characterization of cultured epithelial cells lacking expression of ZO-1. J Biol Chem 279:44785-44794.

43. Vorbrodt, A. W., and D. H. Dobrogowska. 2004. Molecular anatomy of interendothelial junctions in human blood-brain barrier microvessels. Folia Histochem Cytobiol 42:67-75.

44. Bazzoni, G., and E. Dejana. 2004. Endothelial cell-to-cell junctions: molecular organization and role in vascular homeostasis. Physiol Rev 84:869-901.

45. Dejana, E., F. Orsenigo, and M. G. Lampugnani. 2008. The role of adherens junctions and VE-cadherin in the control of vascular permeability. J Cell Sci 121:2115-2122.

46. Dejana, E., and C. Giampietro. 2012. Vascular endothelial-cadherin and vascular stability. Curr Opin Hematol.

47. Taddei, A., C. Giampietro, A. Conti, F. Orsenigo, F. Breviario, V. Pirazzoli, M. Potente, C. Daly, S. Dimmeler, and E. Dejana. 2008. Endothelial adherens junctions control tight junctions by VE-cadherin-mediated upregulation of claudin-5. Nat Cell Biol 10:923-934.

48. Meza, I., G. Ibarra, M. Sabanero, A. Martinez-Palomo, and M. Cereijido. 1980. Occluding junctions and cytoskeletal components in a cultured transporting epithelium. J Cell Biol 87:746-754.

49. Stevenson, B. R., and D. A. Begg. 1994. Concentration-dependent effects of cytochalasin D on tight junctions and actin filaments in MDCK epithelial cells. J Cell Sci 107 ( Pt 3):367-375.

50. Lai, C. H., K. H. Kuo, and J. M. Leo. 2005. Critical role of actin in modulating BBB permeability. Brain Res Brain Res Rev 50:7-13.

51. Moy, A. B., J. Van Engelenhoven, J. Bodmer, J. Kamath, C. Keese, I. Giaever, S. Shasby, and D. M. Shasby. 1996. Histamine and thrombin modulate endothelial focal adhesion through centripetal and centrifugal forces. J Clin Invest 97:1020-1027.

52. Sheldon, R., A. Moy, K. Lindsley, S. Shasby, and D. M. Shasby. 1993. Role of myosin light-chain phosphorylation in endothelial cell retraction. Am J Physiol 265:L606-612.

53. Dudek, S. M., and J. G. Garcia. 2001. Cytoskeletal regulation of pulmonary vascular permeability. J Appl Physiol 91:1487-1500.

54. van Hinsbergh, V. W., and G. P. van Nieuw Amerongen. 2002. Intracellular signalling involved in modulating human endothelial barrier function. J Anat 200:549-560.

55. Vandenbroucke, E., D. Mehta, R. Minshall, and A. B. Malik. 2008. Regulation of endothelial junctional permeability. Ann N Y Acad Sci 1123:134-145.

56. Shen, Q., R. R. Rigor, C. D. Pivetti, M. H. Wu, and S. Y. Yuan. 2010. Myosin light chain kinase in microvascular endothelial barrier function. Cardiovasc Res 87:272-280.

57. Hicks, K., R. G. O'Neil, W. S. Dubinsky, and R. C. Brown. 2010. TRPC-mediated actin-myosin contraction is critical for BBB disruption following hypoxic stress. Am J Physiol Cell Physiol 298:C1583-1593.

58. Ignarro, L. J. 1989. Endothelium-derived nitric oxide: actions and properties. FASEB J 3:31-36.

59. Vanhoutte, P. M. 2009. How We Learned to Say NO. Arterioscler Thromb Vasc Biol 29:1156-1160.

60. Grozdanovic, Z. 2001. NO message from muscle. Microsc Res Tech 55:148-153.

61. Pautz, A., J. Art, S. Hahn, S. Nowag, C. Voss, and H. Kleinert. 2010. Regulation of the expression of inducible nitric oxide synthase. Nitric Oxide 23:75-93.

62. Boje, K. M. 1996. Inhibition of nitric oxide synthase attenuates blood-brain barrier disruption during experimental meningitis. Brain Res 720:75-83.

63. Boueiz, A., and P. M. Hassoun. 2009. Regulation of endothelial barrier function by reactive oxygen and nitrogen species. Microvasc Res 77:26-34.

64. Yuan, S. Y. 2006. New insights into eNOS signaling in microvascular permeability. Am J Physiol Heart Circ Physiol 291:H1029-1031.

65. Takashima, S. 2009. Phosphorylation of myosin regulatory light chain by myosin light chain kinase, and muscle contraction. Circ J 73:208-213.

66. Nag, S. 1991. Protective effect of flunarizine on blood-brain barrier permeability alterations in acutely hypertensive rats. Stroke 22:1265-1269.

67. Brown, R. C., L. Wu, K. Hicks, and G. O'Neil R. 2008. Regulation of blood-brain barrier permeability by transient receptor potential type C and type v calcium-permeable channels. Microcirculation 15:359-371.

68. Abbruscato, T. J., and T. P. Davis. 1999. Combination of hypoxia/aglycemia compromises in vitro blood-brain barrier integrity. J Pharmacol Exp Ther 289:668-675.

69. Langlois, J. A., W. Rutland-Brown, and K. E. Thomas. 2006. Traumatic Brain Injury in the United States: Emergency Department Visits, Hospitalizations, and Deaths. Centers for Disease Control and Prevention, National Center for Injury Prevention and Control.

70. Hardy, W. N., C. D. Foster, M. J. Mason, K. H. Yang, A. I. King, and S. Tashman. 2001. Investigation of Head Injury Mechanisms Using Neutral Density Technology and High-Speed Biplanar X-ray. Stapp Car Crash J 45:337-368.

71. King, A. I., K. H. Yang, L. Zhang, and W. Hardy. 2003. Is Head Injury Caused by Linear or Angular Acceleration? In IRCOBI Conference.

72. Zhang, L., K. H. Yang, and A. I. King. 2001. Biomechanics of neurotrauma. Neurol Res 23:144-156.

73. McLean, A. J., and R. W. G. Anderson. 1997. Biomechanics of Closed Head Injury. In Head Injury. R. P., editor. Chapman & Hall, London.

74. Gaetz, M. 2004. The neurophysiology of brain injury. Clin Neurophysiol 115:4-18.

75. Gennarelli, T. A. 1993. Mechanisms of brain injury. J Emerg Med 11 Suppl 1:5-11.

76. Greve, M. W., and B. J. Zink. 2009. Pathophysiology of traumatic brain injury. Mt Sinai J Med 76:97-104.

77. Unterberg, A. W., J. Stover, B. Kress, and K. L. Kiening. 2004. Edema and brain trauma. Neuroscience 129:1021-1029.

78. Hovda, D. A., D. P. Becker, and Y. Katayama. 1992. Secondary injury and acidosis. J Neurotrauma 9 Suppl 1:S47-60.

79. Weber, J. T. 2004. Calcium homeostasis following traumatic neuronal injury. Curr Neurovasc Res 1:151-171.

80. Fineman, I., D. A. Hovda, M. Smith, A. Yoshino, and D. P. Becker. 1993. Concussive brain injury is associated with a prolonged accumulation of calcium: a 45Ca autoradiographic study. Brain Res 624:94-102.

81. Hofmann, T., M. Schaefer, G. Schultz, and T. Gudermann. 2000. Transient receptor potential channels as molecular substrates of receptor-mediated cation entry. J Mol Med (Berl) 78:14-25.

82. Inoue, R. 2005. TRP channels as a newly emerging non-voltage-gated CA2+ entry channel superfamily. Curr Pharm Des 11:1899-1914.

83. Nilius, B., and T. Voets. 2005. TRP channels: a TR(I)P through a world of multifunctional cation channels. Pflugers Arch 451:1-10.

84. Venkatachalam, K., and C. Montell. 2007. TRP channels. Annu Rev Biochem 76:387-417.

85. Zhang, Y., M. A. Hoon, J. Chandrashekar, K. L. Mueller, B. Cook, D. Wu, C. S. Zuker, and N. J. Ryba. 2003. Coding of sweet, bitter, and umami tastes: different receptor cells sharing similar signaling pathways. Cell 112:293-301.

86. Lee, H., T. Iida, A. Mizuno, M. Suzuki, and M. J. Caterina. 2005. Altered thermal selection behavior in mice lacking transient receptor potential vanilloid 4. J Neurosci 25:1304-1310.

87. Moqrich, A., S. W. Hwang, T. J. Earley, M. J. Petrus, A. N. Murray, K. S. Spencer, M. Andahazy, G. M. Story, and A. Patapoutian. 2005. Impaired

thermosensation in mice lacking TRPV3, a heat and camphor sensor in the skin. Science 307:1468-1472.

88. Caterina, M. J., A. Leffler, A. B. Malmberg, W. J. Martin, J. Trafton, K. R. Petersen-Zeitz, M. Koltzenburg, A. I. Basbaum, and D. Julius. 2000. Impaired nociception and pain sensation in mice lacking the capsaicin receptor. Science 288:306-313.

89. Christensen, A. P., and D. P. Corey. 2007. TRP channels in mechanosensation: direct or indirect activation? Nat Rev Neurosci 8:510-521.

90. Corey, D. P., J. Garcia-Anoveros, J. R. Holt, K. Y. Kwan, S. Y. Lin, M. A. Vollrath, A. Amalfitano, E. L. Cheung, B. H. Derfler, A. Duggan, G. S. Geleoc, P. A. Gray, M. P. Hoffman, H. L. Rehm, D. Tamasauskas, and D. S. Zhang. 2004. TRPA1 is a candidate for the mechanosensitive transduction channel of vertebrate hair cells. Nature 432:723-730.

91. Chachisvilis, M., Y. L. Zhang, and J. A. Frangos. 2006. G protein-coupled receptors sense fluid shear stress in endothelial cells. Proc Natl Acad Sci U S A 103:15463-15468.

92. Haswell, E. S., R. Phillips, and D. C. Rees. 2011. Mechanosensitive channels: what can they do and how do they do it? Structure 19:1356-1369.

93. Singh, P., S. Doshi, J. M. Spaethling, A. J. Hockenberry, T. P. Patel, D. M. Geddes-Klein, D. R. Lynch, and D. F. Meaney. 2012. N-methyl-D-aspartate receptor mechanosensitivity is governed by C terminus of NR2B subunit. J Biol Chem 287:4348-4359.

94. Inoue, R., Z. Jian, and Y. Kawarabayashi. 2009. Mechanosensitive TRP channels in cardiovascular pathophysiology. Pharmacol Ther 123:371-385.

95. Lin, S. Y., and D. P. Corey. 2005. TRP channels in mechanosensation. Curr Opin Neurobiol 15:350-357.

96. Yin, J., and W. M. Kuebler. 2010. Mechanotransduction by TRP channels: general concepts and specific role in the vasculature. Cell Biochem Biophys 56:1-18.

97. Berrout, J., M. Jin, M. Mamenko, O. Zaika, O. Pochynyuk, and R. G. O'Neil. 2012. Function of Transient Receptor Potential Cation Channel Subfamily V Member 4 (TRPV4) as a Mechanical Transducer in Flow-sensitive Segments of Renal Collecting Duct System. J Biol Chem 287:8782-8791.

98. Hartmannsgruber, V., W. T. Heyken, M. Kacik, A. Kaistha, I. Grgic, C. Harteneck, W. Liedtke, J. Hoyer, and R. Kohler. 2007. Arterial response to shear stress critically depends on endothelial TRPV4 expression. PLoS One 2:e827.

99. Liedtke, W., D. M. Tobin, C. I. Bargmann, and J. M. Friedman. 2003. Mammalian TRPV4 (VR-OAC) directs behavioral responses to osmotic and mechanical stimuli in Caenorhabditis elegans. Proc Natl Acad Sci U S A 100 Suppl 2:14531-14536.

100. O'Neil, R. G., and S. Heller. 2005. The mechanosensitive nature of TRPV channels. Pflugers Arch 451:193-203.

101. Wu, L., X. Gao, R. C. Brown, S. Heller, and R. G. O'Neil. 2007. Dual role of the TRPV4 channel as a sensor of flow and osmolality in renal epithelial cells. Am J Physiol Renal Physiol 293:F1699-1713.

102. Giamarchi, A., F. Padilla, B. Coste, M. Raoux, M. Crest, E. Honore, and P. Delmas. 2006. The versatile nature of the calcium-permeable cation channel TRPP2. EMBO Rep 7:787-793.

103. Nauli, S. M., F. J. Alenghat, Y. Luo, E. Williams, P. Vassilev, X. Li, A. E. Elia, W. Lu, E. M. Brown, S. J. Quinn, D. E. Ingber, and J. Zhou. 2003. Polycystins 1 and 2 mediate mechanosensation in the primary cilium of kidney cells. Nat Genet 33:129-137.

104. Sharif-Naeini, R., J. H. Folgering, D. Bichet, F. Duprat, I. Lauritzen, M. Arhatte, M. Jodar, A. Dedman, F. C. Chatelain, U. Schulte, K. Retailleau, L. Loufrani, A. Patel, F. Sachs, P. Delmas, D. J. Peters, and E. Honore. 2009. Polycystin-1 and -2 dosage regulates pressure sensing. Cell 139:587-596.

105. Maroto, R., A. Raso, T. G. Wood, A. Kurosky, B. Martinac, and O. P. Hamill. 2005. TRPC1 forms the stretch-activated cation channel in vertebrate cells. Nat Cell Biol 7:179-185.

106. Alvarez, D. F., J. A. King, and M. I. Townsley. 2005. Resistance to store depletion-induced endothelial injury in rat lung after chronic heart failure. Am J Respir Crit Care Med 172:1153-1160.

107. Tiruppathi, C., M. Freichel, S. M. Vogel, B. C. Paria, D. Mehta, V. Flockerzi, and A. B. Malik. 2002. Impairment of store-operated Ca2+ entry in TRPC4(-/-) mice interferes with increase in lung microvascular permeability. Circ Res 91:70-76.

108. Alvarez, D. F., J. A. King, D. Weber, E. Addison, W. Liedtke, and M. I. Townsley. 2006. Transient receptor potential vanilloid 4-mediated disruption of

the alveolar septal barrier: a novel mechanism of acute lung injury. Circ Res 99:988-995.

109. El Sayed, T., A. Mota, F. Fraternali, and M. Ortiz. 2008. Biomechanics of traumatic brain injury. Comput. Methods Appl. Mech. Engrg. 197:4692-4701.

110. Santo-Domingo, J., and N. Demaurex. 2010. Calcium uptake mechanisms of mitochondria. Biochim Biophys Acta 1797:907-912.

111. Taylor, C. W., D. L. Prole, and T. Rahman. 2009. Ca(2+) channels on the move. Biochemistry 48:12062-12080.

112. Montesano, R., M. S. Pepper, U. Mohle-Steinlein, W. Risau, E. F. Wagner, and L. Orci. 1990. Increased proteolytic activity is responsible for the aberrant morphogenetic behavior of endothelial cells expressing the middle T oncogene. Cell 62:435-445.

113. Brown, R. C., A. P. Morris, and R. G. O'Neil. 2007. Tight junction protein expression and barrier properties of immortalized mouse brain microvessel endothelial cells. Brain Res 1130:17-30.

114. Ellis, E. F., J. S. McKinney, K. A. Willoughby, S. Liang, and J. T. Povlishock. 1995. A new model for rapid stretch-induced injury of cells in culture: characterization of the model using astrocytes. J Neurotrauma 12:325-339.

115. Weber, J. T., B. A. Rzigalinski, K. A. Willoughby, S. F. Moore, and E. F. Ellis. 1999. Alterations in calcium-mediated signal transduction after traumatic injury of cortical neurons. Cell Calcium 26:289-299.

116. Ahmed, S. M., B. A. Rzigalinski, K. A. Willoughby, H. A. Sitterding, and E. F. Ellis. 2000. Stretch-induced injury alters mitochondrial membrane potential

and cellular ATP in cultured astrocytes and neurons. J Neurochem 74:1951-1960.

117. Webster, G. D., B. A. Rzigalinski, and H. C. Gabler. 2008. Development of an improved injury device for neural cell cultures. Biomed Sci Instrum 44:483-488.

118. Grynkiewicz, G., M. Poenie, and R. Y. Tsien. 1985. A new generation of Ca2+ indicators with greatly improved fluorescence properties. J Biol Chem 260:3440-3450.

119. Voets, T., and B. Nilius. 2003. TRPs make sense. J Membr Biol 192:1-8.

120. Watanabe, H., M. Murakami, T. Ohba, Y. Takahashi, and H. Ito. 2008. TRP channel and cardiovascular disease. Pharmacol Ther 118:337-351.

121. Stiber, J. A., M. Seth, and P. B. Rosenberg. 2009. Mechanosensitive channels in striated muscle and the cardiovascular system: not quite a stretch anymore. J Cardiovasc Pharmacol 54:116-122.

122. Bolotina, V. M., S. Najibi, J. J. Palacino, P. J. Pagano, and R. A. Cohen. 1994. Nitric oxide directly activates calcium-dependent potassium channels in vascular smooth muscle. Nature 368:850-853.

123. Cohen, R. A., and T. Adachi. 2006. Nitric-oxide-induced vasodilatation: regulation by physiologic s-glutathiolation and pathologic oxidation of the sarcoplasmic endoplasmic reticulum calcium ATPase. Trends Cardiovasc Med 16:109-114.

124. Yamamoto, S., N. Takahashi, and Y. Mori. 2010. Chemical physiology of oxidative stress-activated TRPM2 and TRPC5 channels. Prog Biophys Mol Biol 103:18-27.

125. Yoshida, T., R. Inoue, T. Morii, N. Takahashi, S. Yamamoto, Y. Hara, M. Tominaga, S. Shimizu, Y. Sato, and Y. Mori. 2006. Nitric oxide activates TRP channels by cysteine S-nitrosylation. Nat Chem Biol 2:596-607.

126. Naumanen, P., P. Lappalainen, and P. Hotulainen. 2008. Mechanisms of actin stress fibre assembly. J Microsc 231:446-454.

127. Pellegrin, S., and H. Mellor. 2007. Actin stress fibres. J Cell Sci 120:3491-3499.

128. Bogatcheva, N. V., and A. D. Verin. 2008. The role of cytoskeleton in the regulation of vascular endothelial barrier function. Microvasc Res 76:202-207.

129. Tavalin, S. J., E. F. Ellis, and L. S. Satin. 1995. Mechanical perturbation of cultured cortical neurons reveals a stretch-induced delayed depolarization. J Neurophysiol 74:2767-2773.

130. McKinney, J. S., K. A. Willoughby, S. Liang, and E. F. Ellis. 1996. Stretch-induced injury of cultured neuronal, glial, and endothelial cells. Effect of polyethylene glycol-conjugated superoxide dismutase. Stroke 27:934-940.

131. Rzigalinski, B. A., J. T. Weber, K. A. Willoughby, and E. F. Ellis. 1998. Intracellular free calcium dynamics in stretch-injured astrocytes. J Neurochem 70:2377-2385.

132. Fukami, K., S. Inanobe, K. Kanemaru, and Y. Nakamura. 2010. Phospholipase C is a key enzyme regulating intracellular calcium and modulating the phosphoinositide balance. Prog Lipid Res 49:429-437.

133. Haorah, J., B. Knipe, S. Gorantla, J. Zheng, and Y. Persidsky. 2007. Alcohol-induced blood-brain barrier dysfunction is mediated via inositol 1,4,5-triphosphate receptor (IP3R)-gated intracellular calcium release. J Neurochem 100:324-336.

134. Ruwhof, C., J. T. van Wamel, L. A. Noordzij, S. Aydin, J. C. Harper, and A. van der Laarse. 2001. Mechanical stress stimulates phospholipase C activity and intracellular calcium ion levels in neonatal rat cardiomyocytes. Cell Calcium 29:73-83.

135. Wang, H., N. Ward, M. Boswell, and D. M. Katz. 2006. Secretion of brain-derived neurotrophic factor from brain microvascular endothelial cells. Eur J Neurosci 23:1665-1670.

136. Jin, M., J. Berrout, L. Chen, and R. G. O'Neil. 2012. Hypotonicity-induced TRPV4 function in renal collecting duct cells: modulation by progressive cross-talk with Ca2+-activated K+ channels. Cell Calcium 51:131-139.

137. Kim, E. Y., C. P. Alvarez-Baron, and S. E. Dryer. 2009. Canonical transient receptor potential channel (TRPC)3 and TRPC6 associate with large-conductance Ca2+-activated K+ (BKCa) channels: role in BKCa trafficking to the surface of cultured podocytes. Mol Pharmacol 75:466-477.

138. Kwan, H. Y., B. Shen, X. Ma, Y. C. Kwok, Y. Huang, Y. B. Man, S. Yu, and X. Yao. 2009. TRPC1 associates with BK(Ca) channel to form a signal complex in vascular smooth muscle cells. Circ Res 104:670-678.

139. Lallet-Daher, H., M. Roudbaraki, A. Bavencoffe, P. Mariot, F. Gackiere, G. Bidaux, R. Urbain, P. Gosset, P. Delcourt, L. Fleurisse, C. Slomianny, E. Dewailly, B. Mauroy, J. L. Bonnal, R. Skryma, and N. Prevarskaya. 2009. Intermediate-conductance Ca2+-activated K+ channels (IKCa1) regulate human prostate cancer cell proliferation through a close control of calcium entry. Oncogene 28:1792-1806.

140. Earley, S., A. L. Gonzales, and R. Crnich. 2009. Endothelium-dependent cerebral artery dilation mediated by TRPA1 and Ca2+-Activated K+ channels. Circ Res 104:987-994.

141. Hu, J., X. Yuan, M. K. Ko, D. Yin, M. R. Sacapano, X. Wang, B. M. Konda, A. Espinoza, K. Prosolovich, J. M. Ong, D. Irvin, and K. L. Black. 2007. Calcium-activated potassium channels mediated blood-brain tumor barrier opening in a rat metastatic brain tumor model. Mol Cancer 6:22.

142. Van Renterghem, C., P. Vigne, and C. Frelin. 1995. A charybdotoxin-sensitive, Ca(2+)-activated K+ channel with inward rectifying properties in brain microvascular endothelial cells: properties and activation by endothelins. J Neurochem 65:1274-1281.

143. Yamazaki, D., H. Kito, S. Yamamoto, S. Ohya, H. Yamamura, K. Asai, and Y. Imaizumi. 2011. Contribution of K(ir)2 potassium channels to ATP-induced cell

death in brain capillary endothelial cells and reconstructed HEK293 cell model. Am J Physiol Cell Physiol 300:C75-86.

144. Kottgen, M., B. Buchholz, M. A. Garcia-Gonzalez, F. Kotsis, X. Fu, M. Doerken, C. Boehlke, D. Steffl, R. Tauber, T. Wegierski, R. Nitschke, M. Suzuki, A. Kramer-Zucker, G. G. Germino, T. Watnick, J. Prenen, B. Nilius, E. W. Kuehn, and G. Walz. 2008. TRPP2 and TRPV4 form a polymodal sensory channel complex. J Cell Biol 182:437-447.

145. Bai, C. X., A. Giamarchi, L. Rodat-Despoix, F. Padilla, T. Downs, L. Tsiokas, and P. Delmas. 2008. Formation of a new receptor-operated channel by heteromeric assembly of TRPP2 and TRPC1 subunits. EMBO Rep 9:472-479.

146. Kobori, T., G. D. Smith, R. Sandford, and J. M. Edwardson. 2009. The transient receptor potential channels TRPP2 and TRPC1 form a heterotetramer with a 2:2 stoichiometry and an alternating subunit arrangement. J Biol Chem 284:35507-35513.

147. Tsiokas, L., T. Arnould, C. Zhu, E. Kim, G. Walz, and V. P. Sukhatme. 1999. Specific association of the gene product of PKD2 with the TRPC1 channel. Proc Natl Acad Sci U S A 96:3934-3939.

148. Zhang, P., Y. Luo, B. Chasan, S. Gonzalez-Perrett, N. Montalbetti, G. A. Timpanaro, R. Cantero Mdel, A. J. Ramos, W. H. Goldmann, J. Zhou, and H. F. Cantiello. 2009. The multimeric structure of polycystin-2 (TRPP2): structural-functional correlates of homo- and hetero-multimers with TRPC1. Hum Mol Genet 18:1238-1251.

149. Haorah, J., D. Heilman, B. Knipe, J. Chrastil, J. Leibhart, A. Ghorpade, D. W. Miller, and Y. Persidsky. 2005. Ethanol-induced activation of myosin light chain kinase leads to dysfunction of tight junctions and blood-brain barrier compromise. Alcohol Clin Exp Res 29:999-1009.

150. Kuhlmann, C. R., R. Tamaki, M. Gamerdinger, V. Lessmann, C. Behl, O. S. Kempski, and H. J. Luhmann. 2007. Inhibition of the myosin light chain kinase prevents hypoxia-induced blood-brain barrier disruption. J Neurochem 102:501-507.

**Vita**

Jonathan Berrout was born in Brownsville, Texas on March 30, 1985, the son of Francis and Juan Berrout. After completing his work at Gladys Porter High School, Brownsville, Texas in 2003, he entered the University of Texas at Brownsville. He received the degree of Bachelor of Arts with a major in biology in May, 2007. In September of 2007 he entered The University of Texas Health Science Center at Houston Graduate School of Biomedical Sciences.

Permanent Address:

225 Windwood Way

Brownsville, TX 78526